



Biogeochemistry of climate driven shifts in Southern Ocean primary producers

Ben J. Fisher¹, Alex J. Poulton², Michael P. Meredith³, Kimberlee Baldry⁴, Oscar Schofield⁵, Sian F. Henley¹.

¹ School of GeoSciences, University of Edinburgh, Edinburgh, United Kingdom

² The Lyell Centre for Earth and Marine Science, Heriot-Watt University, Edinburgh, United Kingdom

³ British Antarctic Survey, Cambridge, United Kingdom

⁴ Institute for Marine and Antarctic Studies, College of Sciences and Engineering, University of Tasmania, Hobart, TAS, Australia

⁵ Center of Ocean Observing Leadership, School of Environmental and Biological Sciences, Rutgers University, New Brunswick, NJ 08901, USA

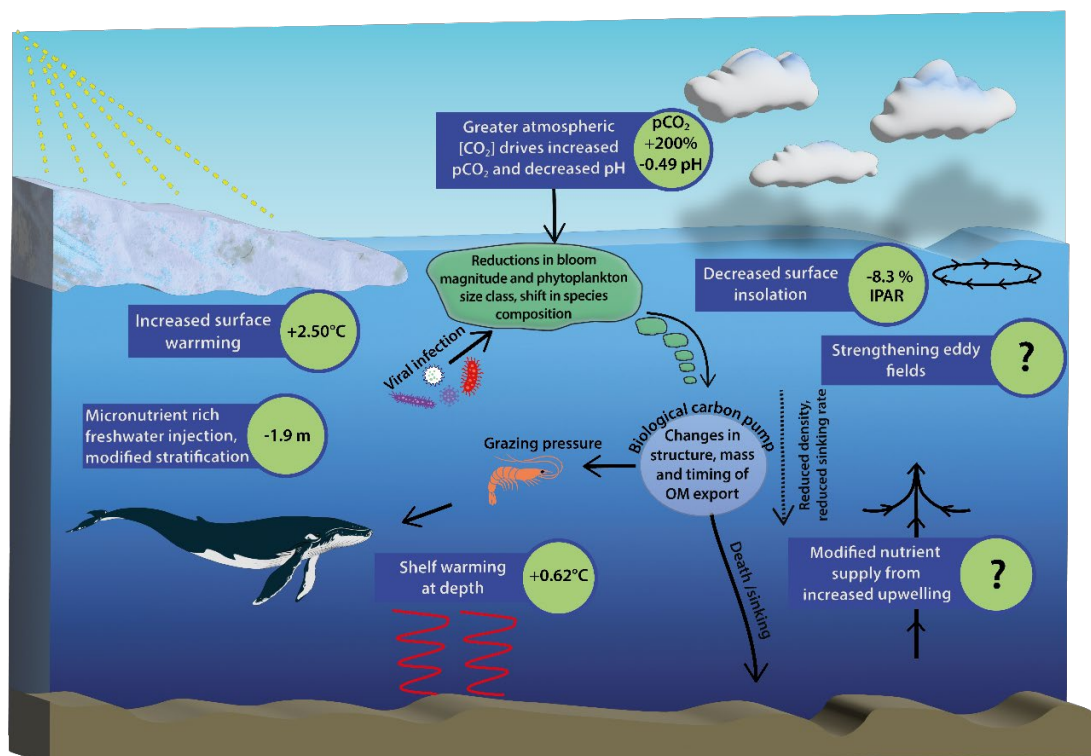
Correspondence to: Ben J. Fisher (ben.fisher@ed.ac.uk)

Abstract. As a net source of nutrients fuelling global primary production, changes in Southern Ocean productivity are expected to influence biological carbon storage across the global ocean. Following a high emission, low mitigation pathway (SSP5-8.5), we show that primary productivity in the Southern Ocean is predicted to increase by up to 30% over the 21st century. The ecophysiological response of marine phytoplankton experiencing climate change will be a key determinant in understanding the impact of Southern Ocean productivity shifts on the carbon cycle. Yet, phytoplankton ecophysiology is poorly represented in Coupled Model Intercomparison 6 (CMIP6) climate models, leading to substantial uncertainty in the representation of their role in carbon sequestration. Here we synthesise the existing spatial and temporal projections of Southern Ocean productivity from CMIP6 models, separated by phytoplankton functional type, and identify key processes where greater observational data coverage can help to improve future model performance. We find substantial variability between models in projections of light concentration ($>15000 \text{ } (\mu\text{E m}^2 \text{ s}^{-1})^2$) across much of the iron and light limited Antarctic zone. Projections of iron and light limitation of phytoplankton vary by up to 10 % across latitudinal zones, while the greatest increases in productivity occurs close to the coast. Temperature, pH and nutrients are less spatially variable, projections for 2090-2100 under SSP5-8.5 show zonally averaged changes of +1.6 °C, -0.45 pH units and Si* decreases by 8.5 $\mu\text{mol L}^{-1}$. Diatoms and pico/misc phytoplankton are equally responsible for driving productivity increases across the Subantarctic and Transitional zones, but pico and misc phytoplankton increase at a greater rate than diatoms in the Antarctic zone. Despite the variability in productivity with different phytoplankton types, we show that the most advanced models disagree on the ecological mechanisms behind these productivity changes. We propose that a sampling approach targeting the regions with the greatest rates of climate-driven change in ocean biogeochemistry and community assemblages would help to resolve the empirical principles underlying phytoplankton community structure in the Southern Ocean.



1. Introduction

The biological uptake of carbon by marine phytoplankton represents an important process in the Earth system (Deppeler and Davidson, 2017), with ocean carbon storage mediating atmospheric CO₂ concentrations, including CO₂ of anthropogenic origin (Riebesell et al., 2007). Across the global ocean, uptake of carbon accounts for ~25% of CO₂ released by human activities (Friedlingstein et al., 2022). The Southern Ocean is a disproportionately large carbon and heat sink relative to its size (Frölicher et al., 2015), accounting for 30-40% of this global anthropogenic CO₂ uptake (e.g. Caldeira and Duffy, 2000; DeVries, 2014), predominantly due to enhanced atmosphere-ocean exchange at increased atmospheric CO₂ concentrations (Friedlingstein et al., 2022). While biological uptake is considered to play a minor role in total CO₂ uptake (Landschützer et al., 2015; Gruber et al., 2019), variability in pCO₂ has been associated with summertime blooms in the Southern Ocean (Gregor et al., 2018; Coggins et al., 2023). Under a future climate scenario with longer growth seasons (Moreau et al., 2015), increased seasonal productivity (Leung et al., 2015; Fu et al., 2016) and a reduction in ocean CO₂ absorption efficiency (higher Revelle factor) (Hauck et al., 2015); biological and physical drivers of carbon exchange across the air-sea interface are likely to undergo substantial changes. As the Southern Ocean's ability to buffer increased concentrations of atmospheric CO₂ weakens, the role of pelagic ecosystems, are expected to become increasingly important in Southern Ocean carbon uptake (Henley et al., 2020).



50 **Figure 1: Schematic diagram of Southern Ocean pressures associated with climate change and the downstream biogeochemical consequences for ecosystem productivity. Values shown are 100 year mean changes to 2100 under the SSP5-8.5 scenario south of 65°S and are taken from CMIP6 models and existing literature (McNeil and Matear, 2008; Purich and England, 2021) (see Table S1 for a full description). Question marks indicate processes where estimations of change do not currently exist.**



Small celled marine phytoplankton (0.002-0.2 mm) are responsible for the production of biological carbon, fuelling ecosystems across the Southern Ocean, but are vulnerable to environmental change because of their specific requirements for light and iron, which are the primary factors limiting their growth in high nutrient low chlorophyll (HNLC) zones of the Southern Ocean (Moore et al., 2013). Following a “middle of the road” SSP2-4.5 pathway, between 2015 and 2023 Southern Ocean phytoplankton (defined as those south of 30°S per Gregg et al. (2003)) represented 36.31% of marine net primary productivity globally, equivalent to 15.5 Pg C yr⁻¹ (Figure S1). Climate impacts on Southern Ocean phytoplankton are likely to manifest in ecological shifts towards smaller cell sizes (Venables et al., 2013; Saba et al., 2014; Schofield et al., 2018; Biggs et al., 2019; Mascioni et al., 2019) and changes in seasonal phenology (Moreau et al., 2015). Increases in overall productivity can be most closely associated with a reduced duration and extent of sea ice coverage, allowing for a greater supply of irradiance to surface waters of this light and iron co-limited productivity system. Strengthened upwelling is also likely to increase the flux of existing iron supplies to the coastal (Annett et al., 2015) and open ocean (Moreau et al., 2023) from sedimentary or hydrothermal sources, however, the extent to which changes in ocean mixing can be expected to impact nutrient supplies remains largely unknown (Figure 1).

Shifts in community composition from diatoms to smaller cryptophytes have already been documented along the West Antarctic Peninsula (Moline et al., 2004; Ducklow et al., 2007; Moline et al., 2008; Montes-Hugo et al., 2008; Rozema et al., 2017), and are thought to be due to tolerance of cryptophytes to the low-salinity waters induced by increased sea ice melt (Moline et al., 2004), or the tolerance of cryptophytes for high and variable light conditions in well stratified surface layers (Mendes et al., 2023). Conversely, in culture-based competition experiments, diatoms are more successful in simulated future ocean conditions over prevalent haptophytes such as *Phaeocystis antarctica*, albeit with reduced diatom cell sizes (Xu et al., 2014). This difference is potentially driven by reduced iron limitation of diatoms and their greater tolerance to temperature change (Zhu et al., 2016). These varied responses between manipulation experiments and *in situ* observations suggest that physiological, as well as ecological, changes are important in understanding the net biogeochemical implications of phytoplankton community change.

In the sea-ice zone, grazing by zooplankton accounts for ~90% of phytoplankton losses (Moreau et al., 2020). Shifts in phytoplankton size class could rapidly cascade through the ecosystem as the dominant Southern Ocean zooplankton, Antarctic krill (*Euphausia superba*, hereafter krill), are unable to graze small cryptophytes (Haberman et al., 2003), instead promoting the dominance of carbon-poor salps (*Salpa thompsoni*), which reduces the overall efficiency of the marine food web (Ballerini et al., 2014) and potentially weakens the biological carbon pump (Quéguiner, 2013; Biggs et al., 2021). Additionally, water temperature, alongside changes to zooplankton abundance and diversity, has been shown to increase zooplankton metabolism (López-Urrutia et al., 2006; Mayzaud and Pakhomov, 2014), which can in turn be expected to modulate the grazing pressure and phytoplankton biomass (Lewandowska et al., 2014).



Projections of productivity in the Southern Ocean under future climate scenarios from the Coupled Model Intercomparison Project Phase 6 (CMIP6) class Earth System Models (ESMs) are actively informing research directions, International Panel on Climate Change (IPCC) reports (Masson-Delmotte et al., 2021), and governmental policy (Touzé-Peiffer et al., 2020). Yet, between CMIP5 and CMIP6 the spread of model projections with respect to vertical and horizontal physics as well as the number of phytoplankton functional types included has increased as different models incorporate more complexity and additional processes (e.g., varying elemental stoichiometry, phytoplankton diversity, complex elemental cycling) (Seferian et al., 2020). While representation of ocean physical drivers and nutrient fields compared to observations has improved between CMIP5 and CMIP6, surface chlorophyll is one of three key parameters that did not show improvement in benchmarking of CMIP6 performance over the global ocean (Canadell et al., 2021;Fu et al., 2022). Variance in model projections of phytoplankton and ocean biogeochemistry have been linked to the use of fixed C:N:P elemental stoichiometry (Kwiatkowski et al., 2018), an inability to reflect physiological adaptations, e.g. the ability of diatoms to maintain growth under iron limitation (Person et al., 2018), and complexities in modelling export fluxes, particularly in constraining phytoplankton losses through zooplankton grazing (Henson et al., 2022).

A major difference in the representation of productivity between CMIP6 models is the extent to which they consider different classes of phytoplankton. Diatoms ($>20\ \mu\text{m}$) and pico-/nano-phytoplankton (predominantly cryptophytes and haptophytes) represent the vast majority of productivity across all latitudes of the Southern Ocean. Diatoms are a significant contributor to primary production and carbon export, accounting for ~40% of global marine primary production and POC exported to depth in the ocean (Jin et al., 2006;Tréguer et al., 2018). Diazotrophs (nitrogen-fixing phytoplankton) are present in small numbers, usually only in subtropical niches, due to the excess supply of nitrogen across the Southern Ocean (Luo et al., 2012). Calcifiers, mostly coccolithophores, inhabit waters north of 60°S where there is a strong supply of light but low Si, high Fe conditions, preventing the growth of diatoms (Charalampopoulou et al., 2016;Nissen et al., 2018). Only 11 CMIP6 models specifically include diatoms under future warming conditions and only three of these additionally consider pico-phytoplankton (CESM2, CESM2-WACCM and GFDL-ESM4).

In recent years, record low sea ice concentrations have been observed in the Southern Ocean (Raphael and Handcock, 2022;Turner et al., 2022). Given the dependence of Southern Ocean productivity on the timing of seasonal sea ice retreat, we consider it possible that this shift in trends of sea ice concentration could cause an abrupt change to sea ice dependent ecosystems in the near future (Swadling et al., 2023). As phytoplankton are the main source of organic carbon in the Southern Ocean, uncertainty in projections of phytoplankton composition compounds existing model uncertainty in the biological carbon flux to the ocean's interior and seafloor (Henson et al., 2022). Within the context of climate change in the Southern Ocean, reducing model uncertainty in ecosystem mediated biogeochemical cycling will be of increased importance in determining the global scale impact of changes in the Southern Ocean productivity regime.



Here we aim to:

1. Quantify the degree of uncertainty between models in projections of phytoplankton productivity with a SSP5-8.5 warming scenario, including different phytoplankton functional types.
- 125 2. Determine mean trends between projected climate driven change in ecosystems, physical processes and biogeochemical cycling across different latitudinal zones of the Southern Ocean.
- 130 3. Identify regions, timeframes and processes within the Southern Ocean Observing System (SOOS) framework (<https://soos.aq>), where the greatest projected changes and/or uncertainties occur. Here, we argue that targeting observations to establish phytoplankton-environment response interactions within the regions of the most rapid projected changes is essential to accelerate the improvement of phytoplankton representation in future generations of ESMs.

2. Methods

Model and observational data for the Southern Ocean were collected and visualised to determine a) the physical and biogeochemical changes that force or result from shifts in productivity, and b) the extent of primary productivity shifts over
135 the next century in CMIP6.

2.1 CMIP projections

Model output was obtained from the Climate Model Intercomparison Project Phase 6 (CMIP6) data server via pangeo.io using the XMIP package in Python 3.11. Ensemble members for each parameter were chosen based on their availability for historical (*hist*) and SSP5-8.5 (*ssp585*) (ScenarioMIP) data (O'Neill et al., 2016). The selected models for each parameter are detailed in
140 Table 1. Where an analysis type relied on the direct comparison between two or more parameters, only models that contained both parameters were selected. For the analysis presented in section 3.5, annual net primary production (*intpp*) is only included from models which also include diatom-specific annual net primary production (*intppdiat*) parameter. Where the same baseline model is included twice, because of having a low- and high-resolution version, the model is pre-averaged (i.e., both resolutions are assigned a weighting of 0.5 each) to avoid double counting of the same model when calculating the ensemble mean.
145 Examples of models with two resolutions are highlighted in bold in Table 1. Only a small number of CMIP6 models contain irradiance limitation (*limirr*) and iron limitation (*limfe*) for multiple phytoplankton types, therefore analyses of light and iron limitation of phytoplankton utilise <5 models. All variables were extracted at monthly frequency, except for surface wind speeds where data were initially obtained daily; subsequently, annual weighted means were generated for most parameters per the weighting algorithm by Grover (2021). For mixed layer depth and incidental photosynthetically active radiation (IPAR),
150 austral summertime means were used instead of annual means.



155 Model data were processed in Python 3.11 to apply the desired analysis (e.g., annual average, annual maximum) and then further averaged over residual variables (e.g., member_id). In most cases, all available member_id's were used; where this was not possible, any member_id's which could not be aggregated due to differences in array structure were removed. Net primary production (NPP) is provided as a pre-integrated value across the water column; we integrated chlorophyll across the depth dimension between 0 and 500 m, to capture all phytoplankton across different depths, using the integrate function in SciPy (Virtanen et al., 2020). Subsequently, all models were re-gridded to a rectilinear grid via bilinear or nearest neighbour interpolation using XESMF (Zhuang et al., 2018) before being averaged to create multi-model means.

160 For spatial plotting, data were projected to the Antarctic Polar Stereographic (EPSG:3031) coordinate reference system in ArcGIS pro and visualised in QGIS using the Quantarctica package (Matsuoka et al., 2021), with post processing using SAGA and GDAL tools to remove imperfections in grid alignment through interpolation. All code to extract the CMIP6 data used in this study is available open access.



Table 1: Selected models used in analysis of CMIP6 data. Models shown in bold represent multiple resolutions of the same core model.

Variable ID	Parameter	Units	Data selection	Models selected
<i>intpp</i>	Primary organic carbon production by all types of phytoplankton	gC m ⁻² yr ⁻¹	Annual average	ACCESS-ESM1-5, CanESM5, CanESM5-CanOE, CESM2 CESM2-WACCM, CMCC-ESM2, CNRM-ESM2-1, EC-Earth3-CC, GFDL-ESM4, GFDL-CM4, IPSL-CM6A-LR, MIROC-ES2L, MPI-ESM1-2-HR , MPI-ESM1-2-LR , MRI-ESM2-0, NorESM2-LM , NorESM2-MM , UKESM1-0-LL
<i>intppdiat</i>	/ diatoms			CanESM5-CanOE, CESM2-WACCM, CNRM-ESM2-1, GFDL-ESM4, IPSL-CM6A-LR, UKESM1-0-LL
<i>chl</i>	Mass concentration of total phytoplankton expressed as chlorophyll in sea water	kg m ⁻³	Annual average	ACCESS-ESM1-5, CanESM5, CanESM5-CanOE, CESM2, CESM2-WACCM, CMCC-ESM2, GFDL-CM4, GFDL-ESM4, MIROC-ES2L, MPI-ESM1-2-HR , MPI-ESM1-2-LR , MRI-ESM2-0, NorESM2-LM , NorESM2-MM , UKESM1-0-LL
<i>limirrpico</i>	Irradiance limitation of	Ratio of growth under environmental irradiance to growth under unlimited irradiance	Annual average	CESM2-WACCM, GFDL-ESM4
<i>limirrmisc</i>	pico-phytoplankton			CanESM5, CNRM-ESM2-1, GFDL-ESM4, IPSL-CM6A-LR
<i>limirrdiat</i>	/			CESM2-WACCM, CNRM-ESM2-1, GFDL-ESM4, IPSL-CM6A-LR, UKESM1-0-LL
<i>limirrdiaz</i>	miscellaneous phytoplankton / diatoms/ diazotrophs			CESM2-WACCM, GFDL-ESM4



<i>limfediatic/misc</i>	Iron limitation of diatoms/picoplankton/miscellaneous phytoplankton	Ratio of growth under environmental iron concentration to growth under unlimited iron concentration	Combined annual average	GFDL-ESM4
<i>rsntds</i>	Net Downward Shortwave Radiation at Sea Water Surface (IPAR)	$W m^{-2}$ (Converted to $\mu E m^{-2} s^{-1}$)	Summertime (daily) maximum	ACCESS-CM2, CanESM5, CanESM5-CanOE, CESM2-WACCM, CMCC-CM2-SR5, CNRM-CM6-1, CNRM-CM6-1-HR , CNRM-ESM2-1, EC-Earth3, EC-Earth3-CC, EC-Earth3-Veg, IPSL-CM6A-LR, MIROC-ES2L, MPI-ESM1-2-HR, MPI-ESM1-2-LR, NorESM2-LM, NorESM2-MM
<i>sfcWindmax</i>	Daily Maximum Near-Surface Wind Speed	$m s^{-1}$	Annual average of daily maxima	AWI-CM-1-1-MR, BCC-CSM2-MR, CanESM5, CMCC-CM2-SR5, CMCC-ESM2, CNRM-CM6-1, CNRM-CM6-1-HR , CNRM-ESM2-1, EC-Earth3, EC-Earth3-CC, EC-Earth3-Veg, EC-Earth3-Veg-LR , GFDL-CM4, HadGEM3-GC31-MM, INM-CM4-8, INM-CM5-0, IPSL-CM6A-LR, KACE-1-0-G, MPI-ESM1-2-HR, MPI-ESM1-2-LR , MRI-ESM2-0, UKESM1-0-LL
<i>mlotst</i>	Ocean Mixed Layer Thickness Defined by σ_t	m	Summertime maximum	ACCESS-CM2, BCC-CSM2-MR, CAMS-CSM1-0, CanESM5, CanESM5-CanOE, CESM2, CESM2-WACCM, CNRM-CM6-1, CNRM-ESM2-1, GFDL-ESM4, GISS-E2-1-G, HadGEM3-GC31-LL, IPSL-CM6A-LR, MPI-ESM1-2-HR, MRI-ESM2-0, NESM3, UKESM1-0-LL
<i>phos</i>	Sea surface pH	pH units	Annual average	CanESM5, CanESM5-CanOE, CESM2, CESM2-WACCM, GFDL-ESM4, IPSL-CM6A-LR, MIROC-ES2L, MRI-ESM2-0, NorESM2-LM



<i>tos</i>	Sea surface temperature	°C	Annual average	ACCESS-CM2, ACCESS-ESM1-5, BCC-CSM2-MR, CAMS-CSM1-0, CanESM5, CanESM5-CanOE, CESM2, CESM2-WACCM, CIesm, CMCC-CM2-SR5, CMCC-ESM2, CNRM-CM6-1, CNRM-CM6-1-HR, CNRM-ESM2-1, E3SM-1-1, EC-Earth3, EC-Earth3-CC, EC-Earth3-Veg, EC-Earth3-Veg-LR, FGOALS-f3-L, FGOALS-g3, FIO-ESM-2-0, GFDL-CM4, GFDL-ESM4, HadGEM3-GC31-LL, HadGEM3-GC31-MM, IITM-ESM, INM-CM4-8, INM-CM5-0, IPSL-CM6A-LR, KACE-1-0-G, KIOST-ESM, MCM-UA-1-0, MIROC6, MIROC-ES2L, MPI-ESM1-2-HR, MPI-ESM1-2-LR, MRI-ESM2-0, NESM3, NorESM2-LM, NorESM2-MM, TaiESM1, UKESM1-0-LL
<i>sios</i>	Surface concentration of silicic acid	$\mu\text{mol L}^{-1}$	Annual average	CanESM5-CanOE, GFDL-ESM4, IPSL-CM6A-LR, MPI-ESM1-2-HR, MPI-ESM1-2-LR, NorESM2-LM, NorESM2-MM, UKESM1-0-LL
<i>no3os</i>	Surface concentration of nitrate	$\mu\text{mol L}^{-1}$	Annual average	CESM2, CESM2-WACCM, GFDL-ESM4, NorESM2-LM, UKESM1-0-LL
<i>limno3</i>	Nitrate limitation of phytoplankton	Ratio of growth under environmental nitrate concentration to growth under unlimited nitrate concentration	Annual average	GFDL-ESM4



2.2 Regional data

Historical concentrations of surface nitrate and silicic acid plus sea surface temperatures were mapped from the World Ocean Atlas 2018 data product (Garcia et al., 2019), representing average values from 1955 to 2017. For Si*, annually averaged data for nitrate and silicic acid were exported at a 1x1 degree resolution and subtracted from one another to produce Si*. To determine Si*, pH and temperature values by SOOS area, SOOS regions south of 55° were drawn as mask layers and subset using the zonal statistics function in QGIS.

3. Results and Discussion

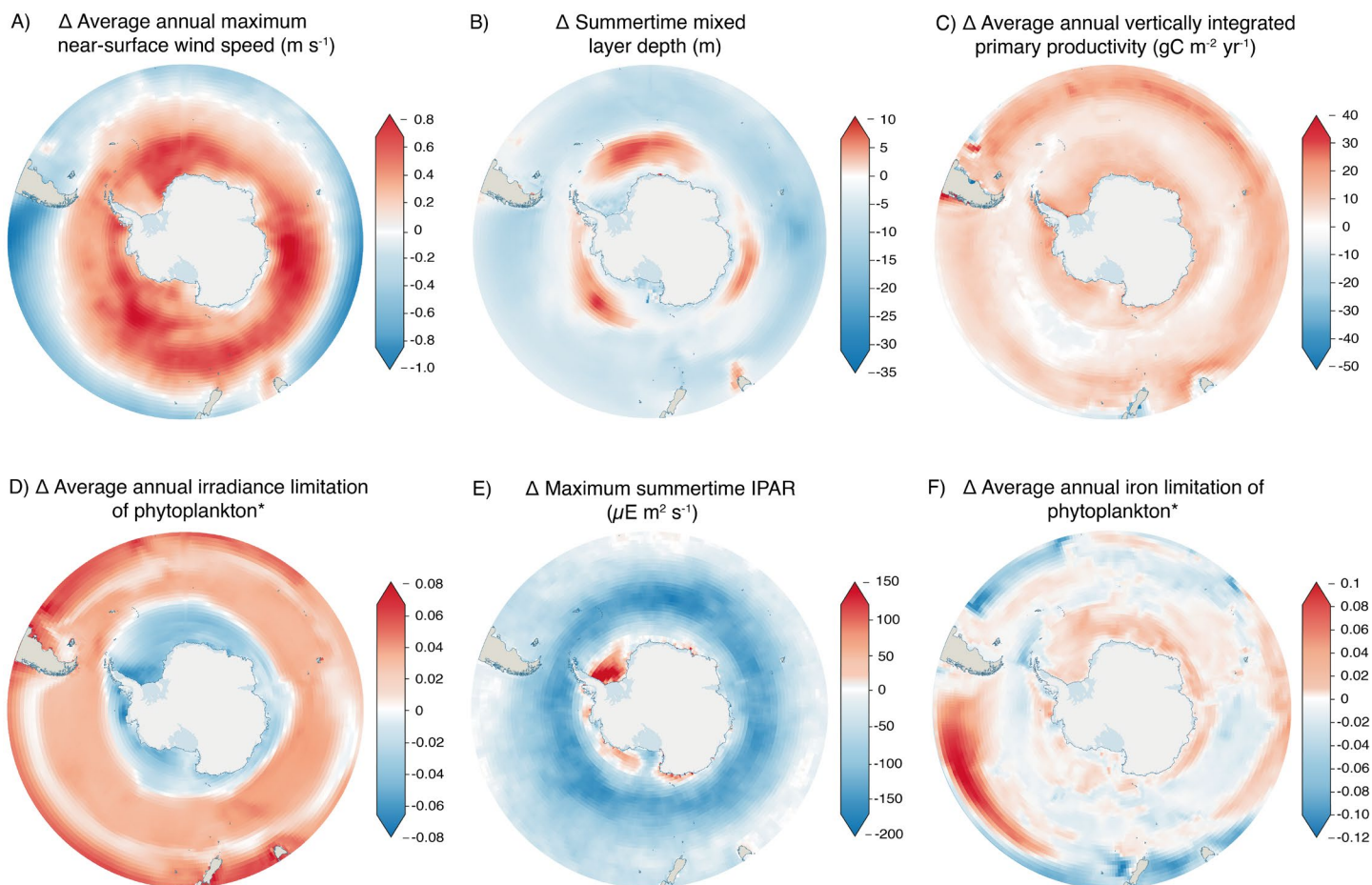
3.1 Physical climate drives biological changes in Southern Ocean water masses

Climate change is driving substantial changes in Southern Ocean water masses (Bindoff et al., 2019). The widespread strengthening of Southern Ocean winds by up to 0.8 m s⁻¹ (Figure 2a) and increased buoyancy fluxes (including freshwater inputs) act as opposing drivers of stratification, modifying mixed layer depth (Figure 2b). Mixed layers are projected to deepen across the Subantarctic by up to 10 m, but shoal across much of the rest of the Southern Ocean (Figure 2b). In light limited regions a shoaling of the mixed layer can be expected to increase productivity, as phytoplankton become concentrated closer to the surface, while in iron limited regions where iron is supplied by wintertime vertical mixing, deeper mixed layers can benefit depth integrated primary productivity by increasing the productive water volume over which iron concentrations are sufficient to promote growth (Llort et al., 2019). Subsequently, the changing availability of light and iron across the Southern Ocean determines the abundance and composition of primary producers. Despite the importance of changes in Southern Ocean circulation for global ocean nutrient supply, the cumulative influence of physical processes across different spatial resolutions results in poor overall performance of CMIP-class models in this region when their historical runs are compared with observations (Meredith et al., 2019). A particular weakness of CMIP6 models is in reconstructing the sea ice changes that drive buoyancy forcing (Roach et al., 2020; Shu et al., 2020) which has an important role in determining the flux of heat and CO₂ across the ocean-atmosphere boundary. The uncertainty in sea ice change also results in a high degree of variation in coastal irradiance between models (Figure S2e), particularly for the Weddell Sea and Ross Sea regions. Recent large and unexpected changes in sea ice around Antarctica emphasise that greater knowledge of the key drivers and controls is required, in order to improve predictive skill in models (Turner and Comiso, 2017).

Across the Southern Ocean, the timing of the springtime onset of net primary production and the magnitude of summer biomass accumulation are controlled by light availability, as dictated by sea ice extent, cloud cover and water column structure (Henley et al., 2017). CMIP6 models project the greatest increase in productivity to occur across the coastal zone of the Southern Ocean (65-90°S) (Figure 2c), where irradiance limitation is reduced (Figure 2d). Conversely, across the Transitional zone (40-50°S),



IPAR reduces (Figure 2e), irradiance limitation increases (Figure 2d) and productivity increases are less here compared to the rest of the Southern Ocean (Figure 2c). Increased iron limitation (Figure 2f) likely manifests from greater competition for iron
200 driven by increased productivity (Figure 2c) despite a potential increase in iron supply with a deepening of the mixed layer across parts of the Subantarctic (50-65°S) (Figure 2b); brought about by reduced upper-ocean stratification from strengthening zonal winds (Carranza and Gille, 2015; Sallee et al., 2021). Iron supply to the surface is subject to changes in the properties and movement of water masses, which lead to variable circulation strengths, depth boundaries, heat content and carbon sequestration resulting from climate-driven perturbations to the ice-ocean-atmosphere system (Bindoff et al., 2019; Meredith
205 et al., 2019). Upwelling of nutrients and light availability for phytoplankton are both strongly influenced by mixed layer depth, which in turn varies seasonally with increased solar warming and ice melt driving deeper Southern Ocean pycnocline stratification through the summer (Sallee et al., 2021). Models generally agree on changes in summertime mixed layer depth across most of the open ocean (Figure S2b), the greatest source of uncertainty is at the terminus of the Ross and Flicher-Ronne ice shelves, inclusion of freshwater input from ice shelves in future CMIP generations could help to reduce uncertainties in
210 stratification.



215 **Figure 2: CMIP6 anomaly representing change to the end of the century in A) near-surface wind speed, B) mixed layer depth, C) net primary productivity, D) irradiance limitation of phytoplankton*, E) incidental photosynthetically active radiation (IPAR), and F) iron limitation of phytoplankton. Changes are calculated from an ensemble of CMIP6 models, comparing a historical (1985-2015) average against 2090-2100 under the SSP5-8.5 climate scenario. Details of ensemble members are given in Table 1. *Units in panels D and F are arbitrary ratios of growth under environmental irradiance or iron concentrations against potential growth under unlimited irradiance or iron concentrations. Positive values represent an increase in limitation, while negative values represent a decrease in limitation.**



220 3.2 Changing biogeochemistry of the Southern Ocean

3.2.1 Micronutrient supply and uptake

Iron acts as the primary limiting nutrient across the Southern Ocean (de Baar et al., 1995; Watson et al., 2000), due to supply limitation from low atmospheric inputs and significant distances from terrigenous sources (Boyd and Ellwood, 2010). Around the Antarctic coast, iron concentrations are set by processes including the resuspension of shelf sediments (Blain et al., 2001),
225 melting of sea ice (Lannuzel et al., 2016) and potential transformation of iron into more labile forms by glacial retreat, as seen in the Arctic (Laufer-Meiser et al., 2021). The change in projected iron limitation of phytoplankton appears minimal (between -12 and 10% Figure 2f). Iron limitation is expected to increase most in the transitional zone between South America and New Zealand, correlating with a reduction in near-surface wind speed (Figure 2a), suggesting that atmospheric deposition of iron will decline in this region. There is a minor increase in iron limitation around the Antarctic coast, which represents the inverse
230 of the decreasing trend in irradiance limitation (Figure 2d), indicating a shift towards an increasingly iron limited system, as reductions in sea ice concentrations increase light availability to coastal waters. The co-occurrence of an increase in iron limitation (Figure 2f) and an increase in total productivity (Figure 2c) across the coastal zone suggests that this increase in limitation is driven by an increase in the uptake of iron (from a larger productivity sink), as opposed to any substantial changes in supply.

235

Despite the importance of iron for phytoplankton growth in the Southern Ocean, CMIP series models have historically struggled to resolve the vertical supply of dissolved iron (Tagliabue et al., 2016), which results in widespread uncertainty for modelling primary and export productivity. At the group level, iron limitation could be expected to influence shifts in phytoplankton communities because larger cells have a greater demand for iron compared to smaller cells. In addition, other
240 micronutrients such as manganese have been identified as a control on phytoplankton growth, particularly during seasonal transitions (Browning et al., 2021). For example, manganese has been shown to play an important role in controlling oxidative stress by catalysing antioxidant production in some diatom species (McCain et al., 2021), explaining the observed phenomenon of iron-manganese co-limitation in the Southern Ocean (Pausch et al., 2019; Browning et al., 2021; Balaguer et al., 2022). Yet only iron is considered in ESMs, due at least partially to the lack of observational data to underpin distribution modelling of
245 other micronutrients. Future work should continue to develop our understanding of the metabolic role of other micronutrients and additionally consider the extent to which diversity exists in micronutrient demand among Southern Ocean phytoplankton species.

3.2.2 Macronutrient supply and uptake

250 Nitrogen species, silicic acid (DSi) and phosphate are all essential for the growth and survival of diatoms, with nitrate and phosphate also being required by all other phytoplankton classes for cellular metabolism. The ratio of utilisation between



nitrogen (N) and phosphorus (P) deviates from the Redfield (1958) ratio of 16:1 across the Southern Ocean according to changes in community composition (Weber and Deutsch, 2010; Henley et al., 2020). Unlike much of the global ocean (Moore et al., 2013), high rates of macronutrient supply from the Circumpolar Deep Water (CDW) prevent widespread N or P
255 limitation in the Southern Ocean except in periods of intense summer growth in high-productivity coastal regions (Henley et al., 2017). Although projections indicate an increase in chlorophyll across such regions (Figure 3), models do not show any increases in nitrate limitation over the remainder of the century (Figure S3), suggesting that iron and light will continue to be the primary constraints on productivity.

260 While macronutrients are not usually limiting to Southern Ocean phytoplankton, growth of diatom communities, particularly around high productivity coastal and island zones (supported by lateral iron advection) (Robinson et al., 2016), is likely to place an increased demand on DSi availability (Table 2). The relationship between Si and N is denoted as Si* ($[\text{Si}(\text{OH})_4] - [\text{NO}_3^-]$) (Sarmiento et al., 2004), with high Si* values (> 25) indicating plentiful DSi availability that supports diatom growth, while low values (< 10) suggest conditions which favour non-silicifying phytoplankton, such as the smaller cryptophytes and
265 haptophytes. Si* is highest in the Antarctic zone (Henley et al., 2020) because of silica input from upwelling of CDW, but remains spatially heterogeneous within this region (Table 2). Si* is consistently high in the Weddell Sea, while across the WAP and Ross, Amundsen and Bellingshausen Seas there is a moderate mean Si* with large variability, and the Indian Sector has a substantially lower DSi availability. Si* is projected to decline by 2090-2100 at a zonally averaged value of $-8.5 \mu\text{mol L}^{-1}$, with the greatest declines being in the Ross and Weddell Seas, as well as the Indian sector (Table 2).

270 Changes in Si* correlate with increases in chlorophyll concentration across the same regions (Figure 3), indicative of increased phytoplankton concentrations resulting in a drawdown of silicic acid. However, increases in chlorophyll appear independent from projected changes in primary productivity (Figure 2c). For example, the west Antarctic Peninsula and Amundsen Sea regions show the greatest increase in primary productivity, but are among the regions of smallest change for both Si* and
275 chlorophyll. The divergence between chlorophyll and primary productivity indicates variability in Chl:C, with siliceous diatoms typically expressing more chlorophyll per unit of carbon (Sathyendranath et al., 2009). Therefore, the large chlorophyll increase and large Si* decline projected in the Weddell Sea is likely driven by an increase in diatoms, whereas the productivity increase with only small changes in both chlorophyll and Si* seen on the west Antarctic Peninsula probably results from an expansion of non-diatom phytoplankton with lower Chl:C.

280 The impact of climate change on DSi supply to the surface is difficult to evaluate because it is dependent on the competing stratification effects from wind driven changes to upwelling and an increase in freshening. Export of DSi from the surface and remineralisation at depth additionally act as important controls on supply; Freeman et al. (2018) showed that increased biological uptake of silicic acid, through increased diatom growth, leads to a poleward shift in the silicic acid front and a
285 potential decoupling from the Antarctic polar front. Efforts to better define the nutrient budgets, particularly in increasingly



common low sea ice years, across different sectors of the Southern Ocean, as well as understanding the changing nutrient demands of phytoplankton will be essential for determining future trends in nutrient limitation (Henley et al., 2019).

3.2.3 Ocean acidification

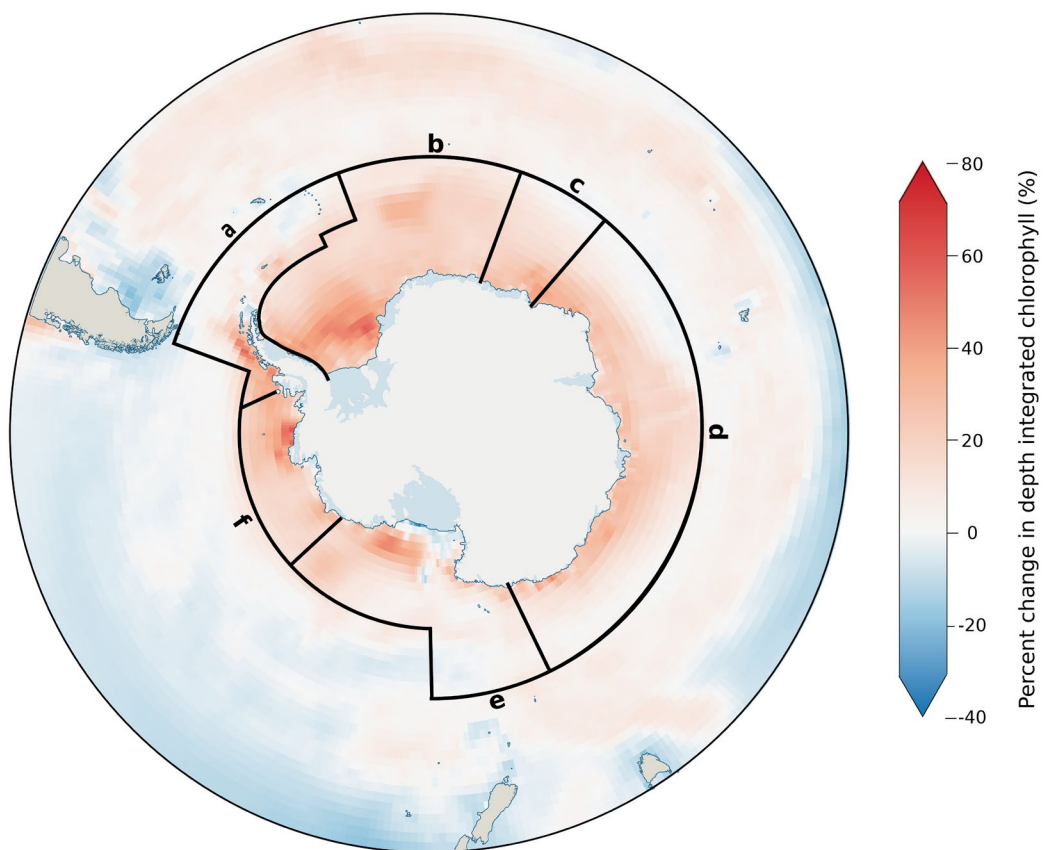
Across all regions of the Southern Ocean, continued uptake of anthropogenic CO₂ is expected to elicit a decrease in surface
290 pH of ~0.45 units south of 55°S (Table 2) under the high emission scenario (SSP5-8.5). Projected changes in pH do not differ regionally, and shows little variation within regions (low standard deviation). This ubiquity in the acidification effect means there no evidence for a direct effect of acidification effect on phytoplankton within our assessment of the Southern Ocean. In the main biogeochemistry modules of CMIP6 members, phytoplankton growth is driven and limited by nutrients and light, while many models are built with complex carbonate systems, these typically only interact with rates of calcification and for
295 the majority of phytoplankton there is no biotic feedback from changes to the carbonate system. Although ocean acidification (OA) is typically considered to have the greatest effect on marine calcifiers through impacts on the production and dissolution of calcium carbonate (Figuerola et al., 2021), OA is also likely to impact diatom (Petrou et al., 2019), pico-phytoplankton (Tortell et al., 2008) and krill (Kawaguchi et al., 2013) populations which form the base of Southern Ocean food webs.

300 When considering species shifts, unravelling the specific impact of OA on individual phytoplankton types is complex due to the fact that OA often acts on phytoplankton indirectly. For example, Petrou et al. (2019) showed that acidification reduces silicification of diatoms (Si:C), likely reducing sinking capacity and increasing rates of remineralisation in the upper ocean, in turn weakening ocean carbon drawdown and acting as a positive feedback on the carbon cycle. Yet in existing CMIP6 biogeochemical modules, silicification is a product of the ambient concentration of either silicic acid (Stock et al., 2020), or
305 silicic acid and iron (Moore et al., 2004), with no interaction from OA. This lack of plasticity might also impact nutrient export rates, Taucher et al., (2022) showed that OA decreases Si dissolution in the surface ocean, resulting in an export flux with a higher Si:N composition. Expanding model setups in CMIP6 to include the impact of OA and other physiochemical drivers on biogeochemical stoichiometry could help to resolve existing biases in Southern Ocean silicic acid concentrations (Long et al., 2021), which has the potential to cause large uncertainty in global NCP due to the role of the Southern Ocean as a net Si
310 source to the global thermohaline circulation. A key challenge in developing our understanding of OA impacts on phytoplankton at the group level is in resolving the mechanistic influence changing acidity has on different phytoplankton. For example, productivity may increase under OA as a result of shifts towards larger diatom species (Tortell et al., 2008). However, some studies have shown that smaller size classes (<20 µm) are more successful at higher pCO₂ values (Hancock et al., 2018) or that total productivity may decrease under OA (Westwood et al., 2018).

315



320



325

330

Figure 3: Change in depth-integrated chlorophyll (0-500 m) from all phytoplankton, displayed as the percentage change between the annual historical average (1985-2015) and projected values for 2090-2100. Values shown are multi-model means of the models listed in Table 1. Spatial boundaries show the Southern Ocean Observing System (SOOS) regions south of 55°S, which are defined in Table 2.



335

Table 2: Biogeochemical parameter values calculated for the Southern Ocean Observing System regions. SOOS regional working groups (as defined at: www.soos.aq/activities/rwg) indicated on Figure 3; section C is an overlap section of sections B and D. Data shown are: Si* ($[\text{Si}(\text{OH})_4] - [\text{NO}_3^-]$) values and temperature determined from objectively analysed annual means of World Ocean Atlas 2018 data. pH was determined from a historical run of a multi-model ensemble of CMIP6 models (1985-2015). Delta values are anomalies of multi-model means of pH, temperature and Si* based on comparisons between the mean annual historical value (1985-2015) and projected values for 2090-2100 under SSP5-8.5 for a CMIP6 ensemble (detailed in Table 1). Values in brackets are standard deviations, representing spatial variation across the region. Anomaly maps for pH, temperature and Si* are shown in Figure S4, S5 and S6 respectively.

Section	SOOS Region	Si* ($\mu\text{mol/L}$)	ΔSi^* ($\mu\text{mol/L}$)	pH	Δ pH	Temperature ($^{\circ}\text{C}$)	Δ Temperature ($^{\circ}\text{C}$)
A	West Antarctic Peninsula & Scotia Arc	17.24 (17.82)	-7.06 (3.63)	8.07 (0.15)	-0.43 (0.01)	1.94 (1.87)	1.79 (0.37)
B	Weddell Sea & Dronning Maud Land (WSDML)	37.37 (9.70)	-10.98 (3.77)	8.08 (0.14)	-0.41 (0.01)	-0.07 (0.95)	1.43 (0.49)
C	SOIS/WSDML	23.16 (6.67)	-8.20 (1.59)	8.07 (0.01)	-0.41 (0.01)	1.08 (1.26)	1.89 (0.40)
D	Southern Ocean Indian Sector (SOIS)	4.71 (3.72)	-10.52 (3.67)	8.07 (0.13)	-0.41 (0.01)	1.78 (1.66)	1.78 (0.46)
E	Ross Sea	19.82 (18.49)	-9.13 (5.02)	8.08 (0.13)	-0.40 (0.02)	0.62 (2.22)	1.08 (0.46)
F	Amundsen and Bellingshausen Seas	17.59 (14.02)	-5.27 (4.33)	8.09 (0.16)	-0.43 (0.01)	0.11 (0.83)	1.73 (0.44)

340

3.3 Primary production and representation in CMIP6

3.3.1 Phytoplankton classes

Two CMIP6 models (GFDL-ESM4 and CESM2-WACCM) showed substantial mechanistic differences in productivity projections by phytoplankton type south of 65°S (Figure 4). While GFDL-ESM4 projects that in this region diatoms account for the majority (55%) of the change in productivity under SSP5-8.5 (Figure 4a,b), diatoms represent only 26% of the productivity increase in CESM2-WACCM, with pico-phytoplankton forming the major (74%) phytoplankton group (Figure

345



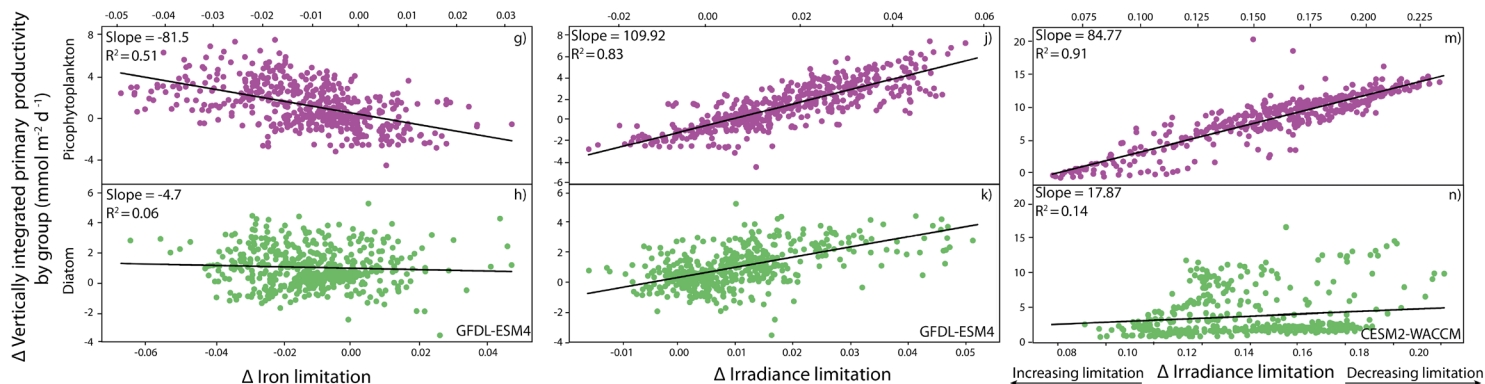
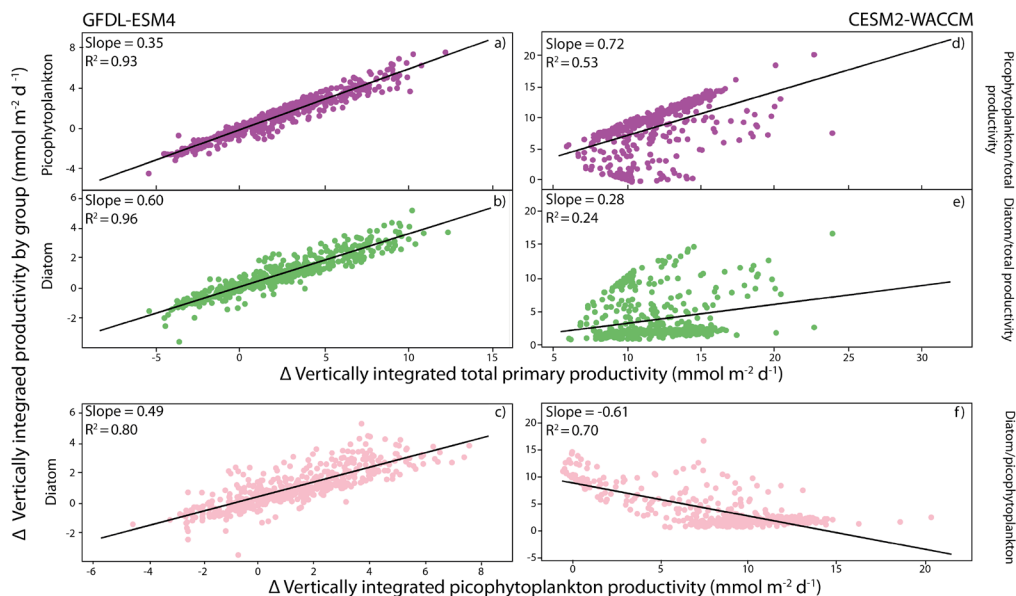
4e,d). Additionally, the GFDL model indicates that increased productivity is driven by increases in both diatoms and pico-phytoplankton, representing a simultaneous growth scenario while CESM2-WACCM favours a replacement mechanism with diatoms decreasing as pico-phytoplankton populations grow (Figure 4c,f). In CESM2-WACCM (MARBL biogeochemistry module) and GFDL-ESM4 (COBALTv2 biogeochemistry module), growth of phytoplankton groups is a product of temperature, nutrient limitation and light availability. In COBALTv2 the iron uptake half saturation constant is greater than in MARBL (0.1 vs 0.03 nmol kg⁻¹ for small phytoplankton) and the differential between small and large phytoplankton (diatom) iron requirements is greater (x5 vs x2.3). Although phytoplankton in MARBL have lower Fe requirements, negative biases towards NO₃⁻ and PO₄⁻³ in the Southern Ocean by CESM2 suggest that NCP is overestimated, subsequently this could drive the system to iron limitation earlier, resulting in an “insufficient contribution from diatoms” (Long et al., 2021). This could suggest that GFDL-ESM4 presents a more realistic outlook for phytoplankton composition, however fixed nutrient constants which usually represent a global average collected from multiple studies, make no differentiation for changes to nutrient uptake in cold water environments. For example, Timmermans et al. (2004) showed iron uptake half saturation values for Southern Ocean diatoms to vary substantially between 0.19 and 1.14 nmol L⁻¹ based on species, compared to a fixed value of 0.5 nmol L⁻¹ for COBALTv2 and 0.07 for MARBL, representing diatoms globally (Stock et al., 2020; Long et al., 2021). Experimentally, uptake half saturation constants are determined through the sequential addition of nutrients, yet multiple studies have shown that Southern Ocean diatoms in particular are able to reduce their cellular iron demand through changes to the photosynthetic pathway (e.g. Strzepek and Harrison, 2004; Jabre et al., 2021). Therefore, models based on these fixed constants may be reflecting the maximal iron uptake rather than the low iron acclimated uptake, i.e., this approach towards modelling nutrient limitation does not allow for a molecular adaptation which can, in some cases, achieve the same growth rate under more limiting conditions.

Key to understanding the ecological and biogeochemical impact of molecular level adaptations will be a shift from single species to community based experiments alongside incorporation of holistic marine ecosystem models which account for an expanded range of biological interactions involved in phytoplankton-zooplankton predation and bacterially-driven mixotrophic effects, which can substantially alter trophic energy transfer and export fluxes (Ward and Follows, 2016). Trait-based approaches have been explored as a means of modelling phytoplankton community composition, distinguishing functional groups based on life histories, morphology and physiology (Litchman and Klausmeier, 2008). Ocean biological sampling has some of the lowest coverage in the Southern Ocean (Sunagawa et al., 2020). Expansion of ecosystem observing at the metagenomics level (e.g., Guidi et al., 2016) offers a promising opportunity to expand our knowledge of traits and trade-offs in Southern Ocean phytoplankton communities, facilitating their integration into climate models.



3.3.2 Ecological dynamics and ecophysiology

In a changing ocean, phytoplankton will succeed where they have the greatest biological plasticity, for example the ability to
380 photo-acclimate rapidly (Arrigo et al., 2010) or scavenge and utilise a diverse range of micronutrients. The physiological
properties of any individual species ultimately determines their ability to survive in a particular region at a particular time
under ever changing climate-driven conditions. Subsequently, species ecology determines the abundance and temporal extent
with which a species can exist or compete in a particular region. As the warming of the climate continues to bring about an
earlier retreat of sea ice, growth seasons are expected to lengthen, altering the temporal dynamics of species progression
385 (Moreau et al., 2015). In the coastal zone of the Southern Ocean, changes in light appear to be the main influence on
productivity with decreased irradiance limitation stimulating pico-phytoplankton growth to a greater extent than diatoms
(Figure 4 j,k,m,n); meanwhile iron limitation shows little correlation with productivity changes in this region (Figure 4 g,h),
likely because of replete iron supplies from coastal upwelling.



390 **Figure 4: Evaluation of GFDL-ESM4 and CESM2-WACCM models using an anomaly between 2090-2100 (SSP5-8.5) and a**
historical average (1985-2015) for the Antarctic zone (65-90°S). Linear regression between change in total productivity and pico-
phytoplankton productivity for GFDL-ESM4 (A) and CESM2-WACCM (D). Linear regression between change in total productivity and
diatom productivity for GFDL-ESM4 (B) and CESM2-WACCM (E). Linear regression between change in picophytoplankton
productivity and diatom productivity for GFDL-ESM4 (C) and CESM2-WACCM (F). Change in iron limitation with
 395 **pico-phytoplankton (G) and diatom (H) productivity for GFDL-ESM4. Change in irradiance limitation with pico-phytoplankton (J)**
and diatom (K) productivity for GFDL-ESM4. Change in irradiance limitation with pico-phytoplankton (M) and diatom (N)
productivity for CESM2-WACCM.



3.4 Latitudinal productivity projections in CMIP6.

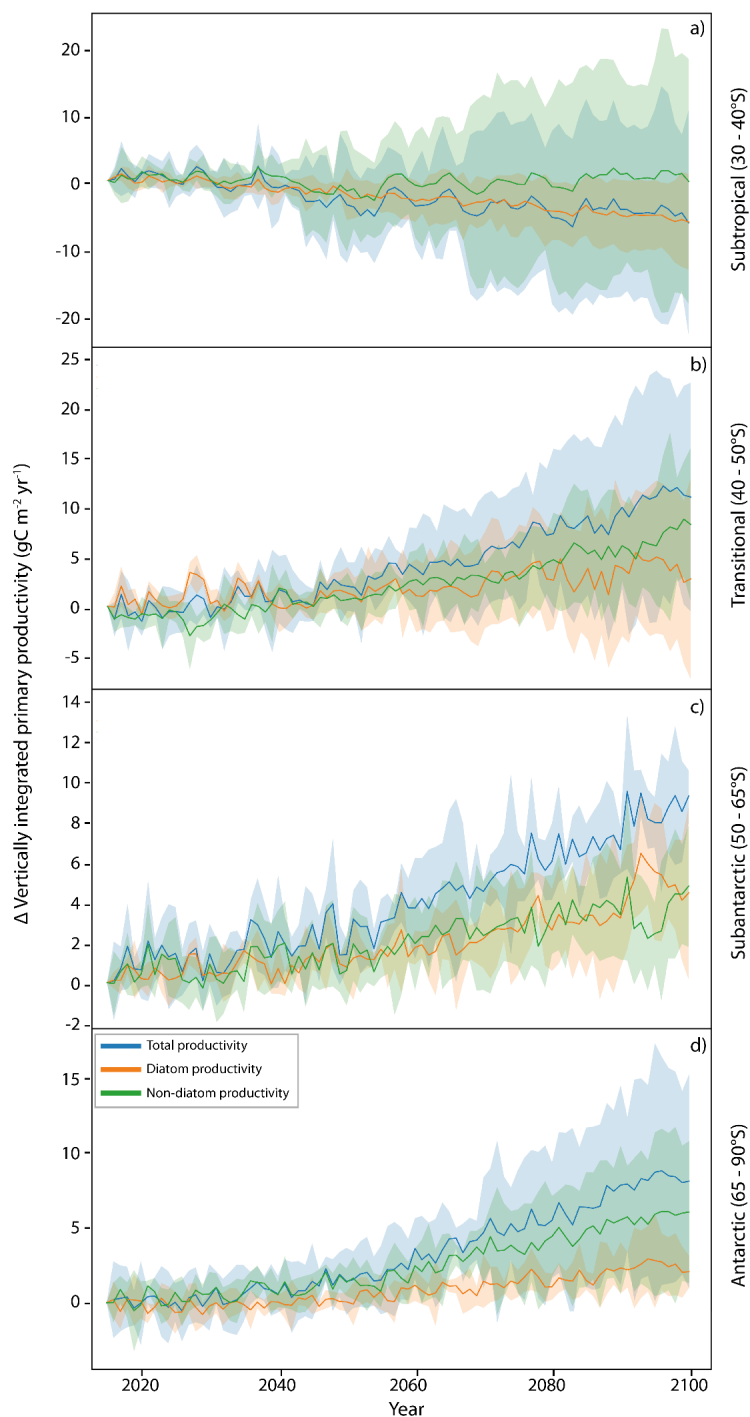
From those models that do distinguish between at least diatoms and other phytoplankton we are able to examine
400 projected changes in community composition over the 21st century under a continued warming scenario (SSP5-
8.5) (Figure 5). Previous analysis by Laufkötter et al. (2015), using a different set of models (a mix of marine
ecosystem models employed in CMIP5 and the Marine Ecosystem Model Intercomparison Project), found
substantial disagreement between models in projecting which phytoplankton groups drove NPP changes in the
Southern Ocean. In CMIP5, Leung et al. (2015) found a latitudinally banded response of phytoplankton to
405 continued warming, driven by the bottom-up dynamics of nitrate, iron and light limitation. From this analysis, we
applied the same latitudinal bands to our analysis of the changes in whole community, diatom and non-diatom
productivity across CMIP6. Our whole community projections agree with the trends shown by Leung et al. (2015),
of a poleward increase in phytoplankton productivity, increasing average total productivity south of 40°S, with
increases in total productivity in the Transitional (40-50°S; Figure 5b), Subantarctic (50-60°S; Figure 5c), and
410 Antarctic zones (65-90°S; Figure 5d). In relative terms, this reflects a ~10% increase in total productivity over the
SSP5-8.5 run (2015-2100) for both the Transitional and Subantarctic zones, with a ~30% increase in productivity
for the Antarctic zone (Figure S7 b,c,d). The poleward increases in productivity correlate with a deepening of
mixed layers around the Antarctic zone (Figure 2b) and a reduction in coastal light limitation (Figure 2d), resulting
in greater increases in Antarctic zone productivity compared to the Transitional or Subantarctic. An ensemble
415 mean shows no overall change in productivity across the Subtropics (see also Tagliabue et al., 2021), however
individual models show the widest degree of divergence in this region, with some models projecting decreases in
the diatom population of over 60% (Figure S7a), indicating a large amount of uncertainty in the magnitude of
productivity changes.

420 In the Subantarctic (50-65°S), despite a large projected increase in light availability (Figure 2e), models project
only a minor increase in productivity driven by a small amount of diatom growth, suggesting that growth of both
diatom and non-diatom species remains largely iron-limited in this region. The coastal zone shows the greatest
degree of change in phytoplankton growth, with the largest increases in this region; the majority of the biomass
change can be attributed to non-diatoms, however relative changes in both diatom and non-diatom populations
425 are similar (Figure S7d), suggesting no overall changes to community composition here. The continued increase
in all phytoplankton classes can be attributed to the decreased iron limitation across much of the zone (Figure 2f),
with the success of non-diatoms reflecting the increase in light limitation (Figure 2d). Large phytoplankton types



are more strongly affected by light limitation in CMIP6 because they have a greater requirement for light (as a lower constant for the chlorophyll specific initial slope of the photosynthesis-irradiance curve), in COBALTv2, large phytoplankton require 3x as much light as small phytoplankton to reach the same rate of photosynthesis (Stock et al., 2020). The lower requirements for iron and light by smaller phytoplankton types means that the change in relative abundance of smaller phytoplankton types to environmental change is often greater compared to diatom populations.

While CMIP6 models do not explicitly consider phytoplankton size, the shift from diatoms to, typically smaller, non-diatom species is consistent with more advanced ecological models such as DARWIN which predict a decrease in the slope of the phytoplankton size spectrum, albeit over a greater area of the Southern Ocean than shown in CMIP6 (Henson et al., 2021). Despite the clear differences between latitudinal bands, spatial heterogeneity continues to exist within these zones, particularly for the coastal zone where some of the greatest increases in chlorophyll occur in the WAP and Weddell Sea regions (Figure 3), reflecting the disproportionately high DSi supply in these regions (Table 2). Resolving spatial heterogeneity of phytoplankton in global-scale models such as those in CMIP6 is likely to require an increased reliance on, and integration with, regional-scale modelling (Person et al., 2018). The rapid increase of non-diatom species around the coast is in agreement with studies describing declining large diatom (>20 μm) abundances (Kang et al., 2001; Wright et al., 2010; Pearce et al., 2011); however, while it is true that diatoms are projected to decrease as a proportion of the community, diatom-derived carbon production is still projected to increase under continued warming, suggesting that the coastal biological carbon pump may be less threatened by this shift in community composition than previously thought.



450 **Figure 5: Changes in productivity ($\text{g C m}^{-2} \text{yr}^{-1}$) and the contribution of different phytoplankton classes to productivity, 2015-2100.**
The anomaly in CMIP6 model productivity projections (as POC production) compared to 2015 for SSP5-8.5 conditions across 4
latitudinal bands of the Southern Ocean, per Leung et al. (2015). Lines represent multi-model means of total productivity (intpp),
diatom productivity (intppdiat) and non-diatom productivity (intpp-intppdiat). Shaded regions represent the spread between
models as the interquartile range. Six CMIP6 models were used in this analysis, because only models containing the diatom
 455 **productivity parameter are included; details of the specific models assessed are given in Table 1.**



4. Conclusions

4.1 Implications of Southern Ocean productivity shifts

The cumulative impact of climate change on phytoplankton has the potential to restructure ecosystems of the Southern Ocean, with wider consequences for global ocean productivity and climate. In this study we found that CMIP6 models project a future Southern Ocean with increased levels of productivity, particularly around the Antarctic coastal zone. The major driver of this is reductions in light limitation, brought about by increased light concentrations from reduced sea ice coverage. However, the extent to which light will change is a source of great uncertainty, with the poor performance of sea ice also having additional implications for buoyancy forcing. Resolving freshwater fluxes from the AIS could reduce model uncertainty in coastal mixed layer depth change. The current iteration of CMIP6 models does not suggest any significant shifts in community composition across the Southern Ocean, outside of a decrease in the relative abundance of diatoms in the subtropics. However, there is a large uncertainty of up to $\pm 30\%$ for all phytoplankton classes across all zones of the Southern Ocean, and key processes which will impact phytoplankton (e.g., viral losses, composition of the grazer community) are absent from most models.

In models which do separate productivity by phytoplankton type, the growth of one type of phytoplankton over another is a product of light, temperature and nutrient limitation. Fixed nutrient stoichiometry is a key limitation in projecting phytoplankton composition, in particular the lack of interaction between physiochemical processes such as OA with biogeochemistry could be responsible for some of the existing biases in models towards excess Si in the Southern Ocean. We showed that for two models (GFDL-ESM4 and CESM2-WACCM) the iron requirements of different phytoplankton types can result in either a simultaneous growth of diatoms and picophytoplankton, or a replacement of diatoms with picophytoplankton. Future model generations might consider the acclimation of diatoms to low iron conditions, models currently use very different uptake half saturation values for iron, which disproportionately impacts community composition in iron limited regions. However, the literature also contains wide divergence in experimentally determined nutrient uptake constants, a more accurate approach towards modelling will first require us to better define what drives this variability in iron requirements. With continued record low sea ice trends, observation of phytoplankton responses in this multi-stressor environment will be essential in understanding the scale of productivity change occurring and provide a basis to incorporate phytoplankton community change into global scale modelling efforts.

4.2 Observational recommendations:

We have identified changes in nutrient upwelling (both upwelling strength and concentration of nutrients at the surface), directionality of mixed layer depth change, mutualism and resource competition between phytoplankton classes, and eddy strengthening as key processes that require improved representation in future generations of climate models. In some cases



490 this is because of lack of monitoring and insufficient data coverage to assess temporal (e.g. seasonal nutrient dynamics) or spatial (e.g. biogeochemical impacts of eddies) variability. While determining the magnitude of MLD change that can be associated with freshwater injection, variability resulting from the relatively recent reversal in Antarctic sea ice trends poses a particular challenge to resolving this process.

Some of the greatest uncertainties in phytoplankton composition exist in diatom abundance between 30°S and 65°S; observationally this may be related to data sparsity, with a greater density of measurements resulting from land-based stations in the coastal zone which has a lower relative uncertainty. However, the existence of a single diatom group in models that consider different phytoplankton functional types could also be limiting here, as subtropical diatoms differ in biology (e.g., 495 lack of ice binding proteins) and species composition compared to polar diatoms. Parameterising these distinct species groups in one functional type inevitably means the model will underperform for some groups relative to others. Monitoring of phytoplankton functional group composition, especially in areas of the greatest projected change (WAP and Weddell Sea), ideally capturing temporally-resolved new productivity in the early spring, will be necessary to detect any changes in 500 community composition. The relationship between chlorophyll, carbon production and Si* appears to be an indicator of community composition, with projected increases in chlorophyll and decreases in Si* in the Weddell Sea indicating a diatom driven increase in productivity. Proxy variables such as these may allow for a coarse determination of community composition from autonomous platforms without the need for personnel intensive microscopy or genomic methods. Crucially, to then link ecological shifts to global climate, the extent to which different phytoplankton species undergo losses via different pathways 505 represents a substantial knowledge gap that needs to be filled to improve the predictive skill of ESMs.

Finally, there is a need for process-based studies including a diverse set of phytoplankton species to further our understanding of fundamental life cycle processes and ecological-biogeochemical coupling. A focus towards defining variability in phytoplankton buoyancy, carbon uptake and release as dissolved organic matter, grazing by zooplankton, interactions with 510 viruses, macronutrient stoichiometry and micronutrient utilisation will enhance our core understanding of Southern Ocean phytoplankton dynamics in a changing climate.

Acknowledgements

BJF is supported by a NERC Doctoral Training Partnership Grant (NE/S007407/1). SFH would like to acknowledge support from NERC (NE/K010034/1). This work used JASMIN, the UK's collaborative data analysis environment 515 (<https://jasmin.ac.uk>). For the purpose of open access, the author has applied a creative commons attribution (CC BY) licence to any author accepted manuscript version arising.



Data availability

CMIP6 data were obtained through, and are freely available at panego.io. Specific models and parameters extracted for each
520 analysis are listed in Table 1. Code for CMIP6 data analysis are available at: (*zenodo link to be later inserted, available to
reviewers as attached zip file*).

Author contributions

BJF, SFH, MPM and AJP devised the concept for the paper and contributed towards initial drafting and editing. BJJ performed
model analysis and produced the figures. OS and KB provided input on conceptual design and edited previous versions of the
525 manuscript. All authors have approved the final version of the manuscript.

Competing interests

The authors declare no competing interests.

References

530 Annett, A. L., Skiba, M., Henley, S. F., Venables, H. J., Meredith, M. P., Statham, P. J., and Ganeshram, R. S.:
Comparative roles of upwelling and glacial iron sources in Ryder Bay, coastal western Antarctic Peninsula,
Marine Chemistry, 176, 21-33, <https://doi.org/10.1016/j.marchem.2015.06.017>, 2015.

Arrigo, K. R., Mills, M. M., Kropuenske, L. R., van Dijken, G. L., Alderkamp, A. C., and Robinson, D. H.:
535 Photophysiology in two major southern ocean phytoplankton taxa: photosynthesis and growth of *Phaeocystis*
antarctica and *Fragilariopsis cylindrus* under different irradiance levels, Integr Comp Biol, 50, 950-966,
10.1093/icb/icq021, 2010.

Balaguer, J., Koch, F., Hassler, C., and Trimborn, S.: Iron and manganese co-limit the growth of two
phytoplankton groups dominant at two locations of the Drake Passage, Commun Biol, 5, 207, 10.1038/s42003-
022-03148-8, 2022.

540 Ballerini, T., Hofmann, E. E., Ainley, D. G., Daly, K., Marrari, M., Ribic, C. A., Smith Jr, W. O., and Steele, J.
H.: Productivity and linkages of the food web of the southern region of the western Antarctic Peninsula
continental shelf, Progress in Oceanography, 122, 10-29, 2014.

Biggs, T. E. G., Alvarez-Fernandez, S., Evans, C., Mojica, K. D. A., Rozema, P. D., Venables, H. J., Pond, D.
W., and Brussaard, C. P. D.: Antarctic phytoplankton community composition and size structure: importance of
545 ice type and temperature as regulatory factors, Polar Biology, 42, 1997-2015, 10.1007/s00300-019-02576-3,
2019.

Biggs, T. E. G., Huisman, J., and Brussaard, C. P. D.: Viral lysis modifies seasonal phytoplankton dynamics and
carbon flow in the Southern Ocean, ISME J, 15, 3615-3622, 10.1038/s41396-021-01033-6, 2021.



- 550 Bindoff, N. L., Cheung, W. W., Kairo, J. G., Arístegui, J., Guinder, V. A., Hallberg, R., Hilmi, N. J. M., Jiao, N., Karim, M. S., and Levin, L.: Changing ocean, marine ecosystems, and dependent communities, IPCC special report on the ocean and cryosphere in a changing climate, 477-587, 2019.
- Blain, S., Tréguer, P., Belviso, S., Bucciarelli, E., Denis, M., Desabre, S., Fiala, M., Jézéquel, V. M., Le Fèvre, J., and Mayzaud, P.: A biogeochemical study of the island mass effect in the context of the iron hypothesis: Kerguelen Islands, Southern Ocean, Deep Sea Research Part I: Oceanographic Research Papers, 48, 163-187, 555 2001.
- Boyd, P. W., and Ellwood, M. J.: The biogeochemical cycle of iron in the ocean, *Nature Geoscience*, 3, 675-682, 10.1038/ngeo964, 2010.
- Browning, T. J., Achterberg, E. P., Engel, A., and Mawji, E.: Manganese co-limitation of phytoplankton growth and major nutrient drawdown in the Southern Ocean, *Nat Commun*, 12, 884, 10.1038/s41467-021-21122-6, 2021.
- 560 Caldeira, K., and Duffy, P. B.: The Role of the Southern Ocean in Uptake and Storage of Anthropogenic Carbon Dioxide, *Science*, 287, 620-622, doi:10.1126/science.287.5453.620, 2000.
- Canadell, J. G., Monteiro, P. M., Costa, M. H., Da Cunha, L. C., Cox, P. M., Alexey, V., Henson, S., Ishii, M., Jaccard, S., Koven, C., Lohila, A., Patra, P. K., Piao, S., Rogelj, J., Syampungani, S., Zaehle, S., and Zickfeld, K.: Global carbon and other Biogeochemical Cycles and Feedbacks, in: *Climate Change 2021: The Physical Science Basis. Contribution of Working Group I to the Sixth Assessment Report of the Intergovernmental Panel on Climate Change* edited by: Masson-Delmotte, V., P. Zhai, A. Pirani, S.L. Connors, C. Péan, S. Berger, N. Caud, Y. Chen, L. Goldfarb, M.I. Gomis, M. Huang, K. Leitzell, E. Lonnoy, J.B.R. Matthews, T.K. Maycock, T. Waterfield, O. Yelekçi, R. Yu, and Zhou, B., Cambridge University Press., In Press, 2021.
- 570 Carranza, M. M., and Gille, S. T.: Southern Ocean wind-driven entrainment enhances satellite chlorophyll-a through the summer, *Journal of Geophysical Research-Oceans*, 120, 304-323, 10.1002/2014jc010203, 2015.
- Charalampopoulou, A., Poulton, A. J., Bakker, D. C. E., Lucas, M. I., Stinchcombe, M. C., and Tyrrell, T.: Environmental drivers of coccolithophore abundance and calcification across Drake Passage (Southern Ocean), *Biogeosciences*, 13, 5917-5935, 10.5194/bg-13-5917-2016, 2016.
- 575 Coggins, A., Watson, A. J., Schuster, U., Mackay, N., King, B., McDonagh, E., and Poulton, A. J.: Surface ocean carbon budget in the 2017 south Georgia diatom bloom: Observations and validation of profiling biogeochemical argo floats, *Deep Sea Research Part II: Topical Studies in Oceanography*, 209, 105275, <https://doi.org/10.1016/j.dsr2.2023.105275>, 2023.
- 580 de Baar, H. J. W., de Jong, J. T. M., Bakker, D. C. E., Löscher, B. M., Veth, C., Bathmann, U., and Smetacek, V.: Importance of iron for plankton blooms and carbon dioxide drawdown in the Southern Ocean, *Nature*, 373, 412-415, 10.1038/373412a0, 1995.
- Deppeler, S. L., and Davidson, A. T.: Southern Ocean Phytoplankton in a Changing Climate, *Frontiers in Marine Science*, 4, ARTN 40 10.3389/fmars.2017.00040, 2017.



- 585 DeVries, T.: The oceanic anthropogenic CO₂ sink: Storage, air-sea fluxes, and transports over the industrial era, *Global Biogeochemical Cycles*, 28, 631-647, 2014.
- Ducklow, H. W., Baker, K., Martinson, D. G., Quetin, L. B., Ross, R. M., Smith, R. C., Stammerjohn, S. E., Vernet, M., and Fraser, W.: Marine pelagic ecosystems: the West Antarctic Peninsula, *Philosophical Transactions of the Royal Society B: Biological Sciences*, 362, 67-94, doi:10.1098/rstb.2006.1955, 2007.
- 590 Figuerola, B., Hancock, A. M., Bax, N., Cummings, V. J., Downey, R., Griffiths, H. J., Smith, J., and Stark, J. S.: A Review and Meta-Analysis of Potential Impacts of Ocean Acidification on Marine Calcifiers From the Southern Ocean, *Frontiers in Marine Science*, 8, 10.3389/fmars.2021.584445, 2021.
- Freeman, N. M., Lovenduski, N. S., Munro, D. R., Krumhardt, K. M., Lindsay, K., Long, M. C., and MacIennan, M.: The Variable and Changing Southern Ocean Silicate Front: Insights From the CESM Large Ensemble, *Global Biogeochemical Cycles*, 32, 752-768, <https://doi.org/10.1029/2017GB005816>, 2018.
- 595 Friedlingstein, P., Jones, M. W., O'Sullivan, M., Andrew, R. M., Bakker, D. C. E., Hauck, J., Le Quéré, C., Peters, G. P., Peters, W., Pongratz, J., Sitch, S., Canadell, J. G., Ciais, P., Jackson, R. B., Alin, S. R., Anthoni, P., Bates, N. R., Becker, M., Bellouin, N., Bopp, L., Chau, T. T. T., Chevallier, F., Chini, L. P., Cronin, M., Currie, K. I., Decharme, B., Djeutchouang, L. M., Dou, X., Evans, W., Feely, R. A., Feng, L., Gasser, T., Gilfillan, D., Gkritzalis, T., Grassi, G., Gregor, L., Gruber, N., Gürses, Ö., Harris, I., Houghton, R. A., Hurtt, G. C., Iida, Y., Ilyina, T., Luijkx, I. T., Jain, A., Jones, S. D., Kato, E., Kennedy, D., Klein Goldewijk, K., Knauer, J., 600 Korsbakken, J. I., Körtzinger, A., Landschützer, P., Lauvset, S. K., Lefèvre, N., Lienert, S., Liu, J., Marland, G., McGuire, P. C., Melton, J. R., Munro, D. R., Nabel, J. E. M. S., Nakaoka, S. I., Niwa, Y., Ono, T., Pierrot, D., Poulter, B., Rehder, G., Resplandy, L., Robertson, E., Rödenbeck, C., Rosan, T. M., Schwinger, J., Schwingshackl, C., Séférian, R., Sutton, A. J., Sweeney, C., Tanhua, T., Tans, P. P., Tian, H., Tilbrook, B., 605 Tubiello, F., van der Werf, G. R., Vuichard, N., Wada, C., Wanninkhof, R., Watson, A. J., Willis, D., Wiltshire, A. J., Yuan, W., Yue, C., Yue, X., Zaehle, S., and Zeng, J.: Global Carbon Budget 2021, *Earth Syst. Sci. Data*, 14, 1917-2005, 10.5194/essd-14-1917-2022, 2022.
- Fripiat, F., Martínez-García, A., Marconi, D., Fawcett, S. E., Kopf, S. H., Luu, V. H., Rafter, P. A., Zhang, R., Sigman, D. M., and Haug, G. H.: Nitrogen isotopic constraints on nutrient transport to the upper ocean, *Nature Geoscience*, 14, 855-861, 10.1038/s41561-021-00836-8, 2021. 610
- Frölicher, T. L., Sarmiento, J. L., Paynter, D. J., Dunne, J. P., Krasting, J. P., and Winton, M.: Dominance of the Southern Ocean in Anthropogenic Carbon and Heat Uptake in CMIP5 Models, *Journal of Climate*, 28, 862-886, 10.1175/jcli-d-14-00117.1, 2015.
- 615 Fu, W., Randerson, J. T., and Moore, J. K.: Climate change impacts on net primary production (NPP) and export production (EP) regulated by increasing stratification and phytoplankton community structure in the CMIP5 models, *Biogeosciences*, 13, 5151-5170, 10.5194/bg-13-5151-2016, 2016.
- Fu, W., Moore, J. K., Primeau, F., Collier, N., Ogunro, O. O., Hoffman, F. M., and Randerson, J. T.: Evaluation of CMIP models with IOMB: Rates of contemporary ocean carbon uptake linked with vertical temperature gradients and transport to the ocean interior, *arXiv preprint arXiv:2202.12933*, 2022.



- 620 Garcia, H., Weathers, K., Paver, C., Smolyar, I., Boyer, T., Locarnini, M., Zweng, M., Mishonov, A., Baranova, O., and Seidov, D.: World ocean atlas 2018. Vol. 4: Dissolved inorganic nutrients (phosphate, nitrate and nitrate+ nitrite, silicate), 2019.
- Gregg, W. W., Conkright, M. E., Ginoux, P., O'Reilly, J. E., and Casey, N. W.: Ocean primary production and climate: Global decadal changes, *Geophysical Research Letters*, 30, <https://doi.org/10.1029/2003GL016889>, 2003.
- 625 2003.
- Gregor, L., Kok, S., and Monteiro, P. M. S.: Interannual drivers of the seasonal cycle of CO₂ in the Southern Ocean, *Biogeosciences*, 15, 2361-2378, 10.5194/bg-15-2361-2018, 2018.
- Correctly calculating annual averages with Xarray: <https://ncar.github.io/esds/posts/2021/yearly-averages-xarray/>, access: 20/01/2024, 2021.
- 630 Gruber, N., Landschützer, P., and Lovenduski, N. S.: The variable Southern Ocean carbon sink, *Annual review of marine science*, 11, 159-186, 2019.
- Guidi, L., Chaffron, S., Bittner, L., Eveillard, D., Larhlimi, A., Roux, S., Darzi, Y., Audic, S., Berline, L., Brum, J. R., Coelho, L. P., Espinoza, J. C. I., Malviya, S., Sunagawa, S., Dimier, C., Kandels-Lewis, S., Picheral, M., Poulain, J., Searson, S., Stemmann, L., Not, F., Hingamp, P., Speich, S., Follows, M., Karp-Boss, L., Boss, E., 635 Ogata, H., Pesant, S., Weissenbach, J., Wincker, P., Acinas, S. G., Bork, P., de Vargas, C., Iudicone, D., Sullivan, M. B., Raes, J., Karsenti, E., Bowler, C., Gorsky, G., and Tara Oceans Consortium, C.: Plankton networks driving carbon export in the oligotrophic ocean, *Nature*, 532, 465-470, 10.1038/nature16942, 2016.
- Haberman, K. L., Ross, R. M., and Quetin, L. B.: Diet of the Antarctic krill (*Dana*): II.: Selective grazing in mixed phytoplankton assemblages, *Journal of Experimental Marine Biology and Ecology*, 283, 97-113, Pii S0022-0981(02)00467-7 640 Doi 10.1016/S0022-0981(02)00467-7, 2003.
- Hancock, A. M., Davidson, A. T., McKinlay, J., McMinn, A., Schulz, K. G., and van den Enden, R. L.: Ocean acidification changes the structure of an Antarctic coastal protistan community, *Biogeosciences*, 15, 2393-2410, 10.5194/bg-15-2393-2018, 2018.
- 645 Hauck, J., Völker, C., Wolf-Gladrow, D. A., Laufkötter, C., Vogt, M., Aumont, O., Bopp, L., Buitenhuis, E. T., Doney, S. C., Dunne, J., Gruber, N., Hashioka, T., John, J., Le Quéré, C., Lima, I. D., Nakano, H., Séférian, R., and Totterdell, I.: On the Southern Ocean CO uptake and the role of the biological carbon pump in the 21st century, *Global Biogeochemical Cycles*, 29, 1451-1470, 10.1002/2015gb005140, 2015.
- 650 Hauck, J., Lenton, A., Langlais, C., and Matear, R.: The Fate of Carbon and Nutrients Exported Out of the Southern Ocean, *Global Biogeochemical Cycles*, 32, 1556-1573, <https://doi.org/10.1029/2018GB005977>, 2018.



- Henley, S. F., Tuerena, R. E., Annett, A. L., Fallick, A. E., Meredith, M. P., Venables, H. J., Clarke, A., and Ganeshram, R. S.: Macronutrient supply, uptake and recycling in the coastal ocean of the west Antarctic Peninsula, *Deep-Sea Res Pt II*, 139, 58-76, [10.1016/j.dsr2.2016.10.003](https://doi.org/10.1016/j.dsr2.2016.10.003), 2017.
- 655 Henley, S. F., Schofield, O. M., Hendry, K. R., Schloss, I. R., Steinberg, D. K., Moffat, C., Peck, L. S., Costa, D. P., Bakker, D. C. E., Hughes, C., Rozema, P. D., Ducklow, H. W., Abele, D., Stefels, J., Van Leeuwe, M. A., Brussaard, C. P. D., Buma, A. G. J., Kohut, J., Sahade, R., Friedlaender, A. S., Stammerjohn, S. E., Venables, H. J., and Meredith, M. P.: Variability and change in the west Antarctic Peninsula marine system: Research priorities and opportunities, *Progress in Oceanography*, 173, 208-237, <https://doi.org/10.1016/j.pcean.2019.03.003>, 2019.
- 660 Henley, S. F., Cavan, E. L., Fawcett, S. E., Kerr, R., Monteiro, T., Sherrell, R. M., Bowie, A. R., Boyd, P. W., Barnes, D. K. A., Schloss, I. R., Marshall, T., Flynn, R., and Smith, S.: Changing Biogeochemistry of the Southern Ocean and Its Ecosystem Implications, *Frontiers in Marine Science*, 7, ARTN 581 [10.3389/fmars.2020.00581](https://doi.org/10.3389/fmars.2020.00581), 2020.
- 665 Henson, S. A., Cael, B. B., Allen, S. R., and Dutkiewicz, S.: Future phytoplankton diversity in a changing climate, *Nat Commun*, 12, 5372, [10.1038/s41467-021-25699-w](https://doi.org/10.1038/s41467-021-25699-w), 2021.
- Henson, S. A., Laufkötter, C., Leung, S., Giering, S. L. C., Palevsky, H. I., and Cavan, E. L.: Uncertain response of ocean biological carbon export in a changing world, *Nature Geoscience*, 15, 248-254, [10.1038/s41561-022-00927-0](https://doi.org/10.1038/s41561-022-00927-0), 2022.
- 670 Jabre, L. J., Allen, A. E., McCain, J. S. P., McCrow, J. P., Tenenbaum, N., Spackeen, J. L., Sipler, R. E., Green, B. R., Bronk, D. A., Hutchins, D. A., and Bertrand, E. M.: Molecular underpinnings and biogeochemical consequences of enhanced diatom growth in a warming Southern Ocean, *Proceedings of the National Academy of Sciences*, 118, e2107238118, [10.1073/pnas.2107238118](https://doi.org/10.1073/pnas.2107238118), 2021.
- 675 Jin, X., Gruber, N., Dunne, J., Sarmiento, J. L., and Armstrong, R.: Diagnosing the contribution of phytoplankton functional groups to the production and export of particulate organic carbon, CaCO₃, and opal from global nutrient and alkalinity distributions, *Global Biogeochemical Cycles*, 20, 2006.
- Kang, S.-H., Kang, J.-S., Lee, S., Chung, K. H., Kim, D., and Park, M. G.: Antarctic phytoplankton assemblages in the marginal ice zone of the northwestern Weddell Sea, *Journal of Plankton Research*, 23, 333-352, 2001.
- 680 Kawaguchi, S., Ishida, A., King, R., Raymond, B., Waller, N., Constable, A., Nicol, S., Wakita, M., and Ishimatsu, A.: Risk maps for Antarctic krill under projected Southern Ocean acidification, *Nature Climate Change*, 3, 843-847, [10.1038/nclimate1937](https://doi.org/10.1038/nclimate1937), 2013.
- Kwiatkowski, L., Aumont, O., Bopp, L., and Ciais, P.: The Impact of Variable Phytoplankton Stoichiometry on Projections of Primary Production, Food Quality, and Carbon Uptake in the Global Ocean, *Global Biogeochemical Cycles*, 32, 516-528, [10.1002/2017gb005799](https://doi.org/10.1002/2017gb005799), 2018.
- 685 Landschützer, P., Gruber, N., Haumann, F. A., Rödenbeck, C., Bakker, D. C. E., Heuven, S. v., Hoppema, M., Metzl, N., Sweeney, C., Takahashi, T., Tilbrook, B., and Wanninkhof, R.: The reinvigoration of the Southern Ocean carbon sink, *Science*, 349, 1221-1224, [doi:10.1126/science.aab2620](https://doi.org/10.1126/science.aab2620), 2015.



- Lannuzel, D., Chever, F., van der Merwe, P. C., Janssens, J., Roukaerts, A., Cavagna, A.-J., Townsend, A. T., Bowie, A. R., and Meiners, K. M.: Iron biogeochemistry in Antarctic pack ice during SIPEX-2, *Deep Sea Research Part II: Topical Studies in Oceanography*, 131, 111-122, <https://doi.org/10.1016/j.dsr2.2014.12.003>, 2016.
- Laufer-Meiser, K., Michaud, A. B., Maisch, M., Byrne, J. M., Kappler, A., Patterson, M. O., Røy, H., and Jørgensen, B. B.: Potentially bioavailable iron produced through benthic cycling in glaciated Arctic fjords of Svalbard, *Nature Communications*, 12, 1349, [10.1038/s41467-021-21558-w](https://doi.org/10.1038/s41467-021-21558-w), 2021.
- 695 Laufkötter, C., Vogt, M., Gruber, N., Aita-Noguchi, M., Aumont, O., Bopp, L., Buitenhuis, E., Doney, S. C., Dunne, J., and Hashioka, T.: Drivers and uncertainties of future global marine primary production in marine ecosystem models, *Biogeosciences*, 12, 6955-6984, 2015.
- Leung, S., Cabré, A., and Marinov, I.: A latitudinally banded phytoplankton response to 21st century climate change in the Southern Ocean across the CMIP5 model suite, *Biogeosciences*, 12, 5715-5734, [10.5194/bg-12-5715-2015](https://doi.org/10.5194/bg-12-5715-2015), 2015.
- 700 Lewandowska, A. M., Hillebrand, H., Lengfellner, K., and Sommer, U.: Temperature effects on phytoplankton diversity — The zooplankton link, *Journal of Sea Research*, 85, 359-364, <https://doi.org/10.1016/j.seares.2013.07.003>, 2014.
- Litchman, E., and Klausmeier, C. A.: Trait-Based Community Ecology of Phytoplankton, *Annual Review of Ecology, Evolution, and Systematics*, 39, 615-639, 2008.
- 705 Llort, J., Lévy, M., Sallée, J. B., and Tagliabue, A.: Nonmonotonic Response of Primary Production and Export to Changes in Mixed-Layer Depth in the Southern Ocean, *Geophysical Research Letters*, 46, 3368-3377, <https://doi.org/10.1029/2018GL081788>, 2019.
- Long, M. C., Moore, J. K., Lindsay, K., Levy, M., Doney, S. C., Luo, J. Y., Krumhardt, K. M., Letscher, R. T., Grover, M., and Sylvester, Z. T.: Simulations With the Marine Biogeochemistry Library (MARBL), *Journal of Advances in Modeling Earth Systems*, 13, e2021MS002647, <https://doi.org/10.1029/2021MS002647>, 2021.
- 710 López-Urrutia, Á., San Martín, E., Harris, R. P., and Irigoien, X.: Scaling the metabolic balance of the oceans, *Proceedings of the National Academy of Sciences*, 103, 8739-8744, doi:10.1073/pnas.0601137103, 2006.
- Luo, Y.-W., Doney, S., Anderson, L., Benavides, M., Berman-Frank, I., Bode, A., Bonnet, S., Boström, K. H., Böttjer, D., and Capone, D.: Database of diazotrophs in global ocean: abundance, biomass and nitrogen fixation rates, *Earth System Science Data*, 4, 47-73, 2012.
- 715 Mascioni, M., Almandoz, G. O., Cefarelli, A. O., Cusick, A., Ferrario, M. E., and Vernet, M.: Phytoplankton composition and bloom formation in unexplored nearshore waters of the western Antarctic Peninsula, *Polar Biology*, 42, 1859-1872, [10.1007/s00300-019-02564-7](https://doi.org/10.1007/s00300-019-02564-7), 2019.
- 720 Masson-Delmotte, V., Zhai, P., Pirani, A., Connors, S. L., Péan, C., Berger, S., Caud, N., Chen, Y., Goldfarb, L., and Gomis, M.: Climate change 2021: the physical science basis, Contribution of working group I to the sixth assessment report of the intergovernmental panel on climate change, 2, 2021.



- Matsuoka, K., Skoglund, A., Roth, G., de Pomereu, J., Griffiths, H., Headland, R., Herried, B., Katsumata, K., Le Brocq, A., Licht, K., Morgan, F., Neff, P. D., Ritz, C., Scheinert, M., Tamura, T., Van de Putte, A., van den Broeke, M., von Deschwandern, A., Deschamps-Berger, C., Van Liefferinge, B., Tronstad, S., and Melvær, Y.: Quantarctica, an integrated mapping environment for Antarctica, the Southern Ocean, and sub-Antarctic islands, *Environmental Modelling & Software*, 140, 105015, <https://doi.org/10.1016/j.envsoft.2021.105015>, 2021.
- 725
- Mayzaud, P., and Pakhomov, E. A.: The role of zooplankton communities in carbon recycling in the Ocean: the case of the Southern Ocean, *Journal of Plankton Research*, 36, 1543-1556, 10.1093/plankt/fbu076, 2014.
- 730
- McCain, J. S. P., Tagliabue, A., Susko, E., Achterberg, E. P., Allen, A. E., and Bertrand, E. M.: Cellular costs underpin micronutrient limitation in phytoplankton, *Science Advances*, 7, eabg6501, 10.1126/sciadv.abg6501, 2021.
- McNeil, B. I., and Matear, R. J.: Southern Ocean acidification: A tipping point at 450-ppm atmospheric CO₂, *Proceedings of the National Academy of Sciences*, 105, 18860-18864, 2008.
- 735
- Mendes, C. R. B., Costa, R. R., Ferreira, A., Jesus, B., Tavano, V. M., Dotto, T. S., Leal, M. C., Kerr, R., Islabao, C. A., Franco, A., Mata, M. M., Garcia, C. A. E., and Secchi, E. R.: Cryptophytes: An emerging algal group in the rapidly changing Antarctic Peninsula marine environments, *Glob Chang Biol*, 29, 1791-1808, 10.1111/gcb.16602, 2023.
- Meredith, M., Sommerkorn, M., Cassotta, S., Derksen, C., Ekaykin, A., Hollowed, A., Kofinas, G., Mackintosh, A., Melbourne-Thomas, J., and Muelbert, M.: Chapter 3: polar regions, IPCC special report on the ocean and cryosphere in a changing climate, 5, 2019.
- 740
- Moline, M. A., Claustre, H., Frazer, T. K., Schofield, O., and Vernet, M.: Alteration of the food web along the Antarctic Peninsula in response to a regional warming trend, *Global Change Biology*, 10, 1973-1980, 10.1111/j.1365-2486.2004.00825.x, 2004.
- 745
- Moline, M. A., Karnovsky, N. J., Brown, Z., Divoky, G. J., Frazer, T. K., Jacoby, C. A., Torres, J. J., and Fraser, W. R.: High latitude changes in ice dynamics and their impact on polar marine ecosystems, *Annals of the New York Academy of Sciences*, 1134, 267, 2008.
- Montes-Hugo, M., Vernet, M., Martinson, D., Smith, R., and Iannuzzi, R.: Variability on phytoplankton size structure in the western Antarctic Peninsula (1997–2006), *Deep Sea Research Part II: Topical Studies in Oceanography*, 55, 2106-2117, 2008.
- 750
- Moore, C. M., Mills, M. M., Arrigo, K. R., Berman-Frank, I., Bopp, L., Boyd, P. W., Galbraith, E. D., Geider, R. J., Guieu, C., Jaccard, S. L., Jickells, T. D., La Roche, J., Lenton, T. M., Mahowald, N. M., Marañón, E., Marinov, I., Moore, J. K., Nakatsuka, T., Oschlies, A., Saito, M. A., Thingstad, T. F., Tsuda, A., and Ulloa, O.: Processes and patterns of oceanic nutrient limitation, *Nature Geoscience*, 6, 701-710, 10.1038/Ngeo1765, 2013.
- 755
- Moore, J. K., Doney, S. C., and Lindsay, K.: Upper ocean ecosystem dynamics and iron cycling in a global three-dimensional model, *Global Biogeochemical Cycles*, 18, <https://doi.org/10.1029/2004GB002220>, 2004.



- Moore, J. K., Fu, W., Primeau, F., Britten, G. L., Lindsay, K., Long, M., Doney, S. C., Mahowald, N., Hoffman, F., and Randerson, J. T.: Sustained climate warming drives declining marine biological productivity, *Science*, 359, 1139-1143, 2018.
- 760 Moreau, S., Mostajir, B., Bélanger, S., Schloss, I. R., Vancoppenolle, M., Demers, S., and Ferreyra, G. A.: Climate change enhances primary production in the western Antarctic Peninsula, *Global Change Biology*, 21, 2191-2205, <https://doi.org/10.1111/gcb.12878>, 2015.
- Moreau, S., Boyd, P. W., and Strutton, P. G.: Remote assessment of the fate of phytoplankton in the Southern Ocean sea-ice zone, *Nat Commun*, 11, 3108, 10.1038/s41467-020-16931-0, 2020.
- 765 Moreau, S., Hattermann, T., de Steur, L., Kauko, H. M., Ahonen, H., Ardelan, M., Assmy, P., Chierici, M., Descamps, S., Dinter, T., Falkenhaus, T., Fransson, A., Gronningsaeter, E., Hallfredsson, E. H., Huhn, O., Lebrun, A., Lowther, A., Lubcker, N., Monteiro, P., Peeken, I., Roychoudhury, A., Rozanska, M., Ryan-Keogh, T., Sanchez, N., Singh, A., Simonsen, J. H., Steiger, N., Thomalla, S. J., van Tonder, A., Wiktor, J. M., and Steen, H.: Wind-driven upwelling of iron sustains dense blooms and food webs in the eastern Weddell Gyre, *Nat Commun*, 14, 1303, 10.1038/s41467-023-36992-1, 2023.
- 770 Nissen, C., Vogt, M., Münnich, M., Gruber, N., and Haumann, F. A.: Factors controlling coccolithophore biogeography in the Southern Ocean, *Biogeosciences*, 15, 6997-7024, 10.5194/bg-15-6997-2018, 2018.
- Nissen, C., Gruber, N., Münnich, M., and Vogt, M.: Southern Ocean Phytoplankton Community Structure as a Gatekeeper for Global Nutrient Biogeochemistry, *Global Biogeochemical Cycles*, 35, e2021GB006991, ARTN e2021GB006991
- 775 10.1029/2021GB006991, 2021.
- O'Neill, B. C., Tebaldi, C., van Vuuren, D. P., Eyring, V., Friedlingstein, P., Hurtt, G., Knutti, R., Kriegler, E., Lamarque, J. F., Lowe, J., Meehl, G. A., Moss, R., Riahi, K., and Sanderson, B. M.: The Scenario Model Intercomparison Project (ScenarioMIP) for CMIP6, *Geosci. Model Dev.*, 9, 3461-3482, 10.5194/gmd-9-3461-2016, 2016.
- 780 Palter, J. B., Sarmiento, J. L., Gnanadesikan, A., Simeon, J., and Slater, R. D.: Fueling export production: nutrient return pathways from the deep ocean and their dependence on the Meridional Overturning Circulation, *Biogeosciences*, 7, 3549-3568, 10.5194/bg-7-3549-2010, 2010.
- Pausch, F., Bischof, K., and Trimborn, S.: Iron and manganese co-limit growth of the Southern Ocean diatom *Chaetoceros debilis*, *PLoS One*, 14, e0221959, 10.1371/journal.pone.0221959, 2019.
- 785 Pearce, I., Davidson, A. T., Thomson, P. G., Wright, S., and van den Enden, R.: Marine microbial ecology in the sub-Antarctic Zone: Rates of bacterial and phytoplankton growth and grazing by heterotrophic protists, *Deep Sea Research Part II: Topical Studies in Oceanography*, 58, 2248-2259, 2011.
- Person, R., Aumont, O., and Lévy, M.: The Biological Pump and Seasonal Variability of pCO₂ in the Southern Ocean: Exploring the Role of Diatom Adaptation to Low Iron, *Journal of Geophysical Research-Oceans*, 123, 3204-3226, 10.1029/2018jc013775, 2018.
- 790



- Petrou, K., Baker, K. G., Nielsen, D. A., Hancock, A. M., Schulz, K. G., and Davidson, A. T.: Acidification diminishes diatom silica production in the Southern Ocean, *Nature Climate Change*, 9, 781-786, [10.1038/s41558-019-0557-y](https://doi.org/10.1038/s41558-019-0557-y), 2019.
- 795 Primeau, F. W., Holzer, M., and DeVries, T.: Southern Ocean nutrient trapping and the efficiency of the biological pump, *Journal of Geophysical Research: Oceans*, 118, 2547-2564, <https://doi.org/10.1002/jgrc.20181>, 2013.
- Purich, A., and England, M. H.: Historical and Future Projected Warming of Antarctic Shelf Bottom Water in CMIP6 Models, *Geophysical Research Letters*, 48, e2021GL092752, <https://doi.org/10.1029/2021GL092752>,
800 2021.
- Quéguiner, B.: Iron fertilization and the structure of planktonic communities in high nutrient regions of the Southern Ocean, *Deep Sea Research Part II: Topical Studies in Oceanography*, 90, 43-54, <https://doi.org/10.1016/j.dsr2.2012.07.024>, 2013.
- Raphael, M. N., and Handcock, M. S.: A new record minimum for Antarctic sea ice, *Nature Reviews Earth & Environment*, 3, 215-216, [10.1038/s43017-022-00281-0](https://doi.org/10.1038/s43017-022-00281-0), 2022.
805
- Redfield, A. C.: The biological control of chemical factors in the environment, *American scientist*, 46, 230A-221, 1958.
- Riebesell, U., Schulz, K. G., Bellerby, R. G. J., Botros, M., Fritsche, P., Meyerhöfer, M., Neill, C., Nondal, G., Oeschies, A., Wohlers, J., and Zöllner, E.: Enhanced biological carbon consumption in a high CO₂ ocean, *Nature*,
810 450, 545-548, [10.1038/nature06267](https://doi.org/10.1038/nature06267), 2007.
- Roach, L. A., Dörr, J., Holmes, C. R., Massonnet, F., Blockley, E. W., Notz, D., Rackow, T., Raphael, M. N., O'Farrell, S. P., Bailey, D. A., and Bitz, C. M.: Antarctic Sea Ice Area in CMIP6, *Geophysical Research Letters*, 47, e2019GL086729, <https://doi.org/10.1029/2019GL086729>, 2020.
- Rozema, P. D., Venables, H. J., van de Poll, W. H., Clarke, A., Meredith, M. P., and Buma, A. G. J.: Interannual variability in phytoplankton biomass and species composition in northern Marguerite Bay (West Antarctic Peninsula) is governed by both winter sea ice cover and summer stratification, *Limnology and Oceanography*, 62, 235-252, <https://doi.org/10.1002/lno.10391>, 2017.
815
- Saba, G. K., Fraser, W. R., Saba, V. S., Iannuzzi, R. A., Coleman, K. E., Doney, S. C., Ducklow, H. W., Martinson, D. G., Miles, T. N., Patterson-Fraser, D. L., Stammerjohn, S. E., Steinberg, D. K., and Schofield, O.
820 M.: Winter and spring controls on the summer food web of the coastal West Antarctic Peninsula, *Nat Commun*, 5, 4318, [10.1038/ncomms5318](https://doi.org/10.1038/ncomms5318), 2014.
- Sallee, J. B., Pellichero, V., Akhoudas, C., Pauthenet, E., Vignes, L., Schmidtke, S., Garabato, A. N., Sutherland, P., and Kuusela, M.: Summertime increases in upper-ocean stratification and mixed-layer depth, *Nature*, 591, 592-598, [10.1038/s41586-021-03303-x](https://doi.org/10.1038/s41586-021-03303-x), 2021.
- 825 Sarmiento, J. L., Gruber, N., Brzezinski, M. A., and Dunne, J. P.: High-latitude controls of thermocline nutrients and low latitude biological productivity, *Nature*, 427, 56-60, [10.1038/nature02127](https://doi.org/10.1038/nature02127), 2004.



- Sathyendranath, S., Stuart, V., Nair, A., Oka, K., Nakane, T., Bouman, H., Forget, M.-H., Maass, H., and Platt, T.: Carbon-to-chlorophyll ratio and growth rate of phytoplankton in the sea, *Marine Ecology Progress Series*, 383, 73-84, 2009.
- 830 Schofield, O., Brown, M., Kohut, J., Nardelli, S., Saba, G., Waite, N., and Ducklow, H.: Changes in the upper ocean mixed layer and phytoplankton productivity along the West Antarctic Peninsula, *Philosophical Transactions of the Royal Society A: Mathematical, Physical and Engineering Sciences*, 376, 20170173, doi:10.1098/rsta.2017.0173, 2018.
- 835 Seferian, R., Berthet, S., Yool, A., Palmieri, J., Bopp, L., Tagliabue, A., Kwiatkowski, L., Aumont, O., Christian, J., Dunne, J., Gehlen, M., Ilyina, T., John, J. G., Li, H., Long, M. C., Luo, J. Y., Nakano, H., Romanou, A., Schwinger, J., Stock, C., Santana-Falcon, Y., Takano, Y., Tjiputra, J., Tsujino, H., Watanabe, M., Wu, T., Wu, F., and Yamamoto, A.: Tracking Improvement in Simulated Marine Biogeochemistry Between CMIP5 and CMIP6, *Curr Clim Change Rep*, 6, 95-119, 10.1007/s40641-020-00160-0, 2020.
- 840 Shu, Q., Wang, Q., Song, Z., Qiao, F., Zhao, J., Chu, M., and Li, X.: Assessment of Sea Ice Extent in CMIP6 With Comparison to Observations and CMIP5, *Geophysical Research Letters*, 47, e2020GL087965, <https://doi.org/10.1029/2020GL087965>, 2020.
- 845 Stock, C. A., Dunne, J. P., Fan, S., Ginoux, P., John, J., Krasting, J. P., Laufkötter, C., Paulot, F., and Zadeh, N.: Ocean Biogeochemistry in GFDL's Earth System Model 4.1 and Its Response to Increasing Atmospheric CO₂, *Journal of Advances in Modeling Earth Systems*, 12, e2019MS002043, <https://doi.org/10.1029/2019MS002043>, 2020.
- Strzepek, R. F., and Harrison, P. J.: Photosynthetic architecture differs in coastal and oceanic diatoms, *Nature*, 431, 689-692, 10.1038/nature02954, 2004.
- 850 Sunagawa, S., Acinas, S. G., Bork, P., Bowler, C., Acinas, S. G., Babin, M., Bork, P., Boss, E., Bowler, C., Cochrane, G., de Vargas, C., Follows, M., Gorsky, G., Grimsley, N., Guidi, L., Hingamp, P., Iudicone, D., Jaillon, O., Kandels, S., Karp-Boss, L., Karsenti, E., Lescot, M., Not, F., Ogata, H., Pesant, S., Poulton, N., Raes, J., Sardet, C., Sieracki, M., Speich, S., Stemann, L., Sullivan, M. B., Sunagawa, S., Wincker, P., Eveillard, D., Gorsky, G., Guidi, L., Iudicone, D., Karsenti, E., Lombard, F., Ogata, H., Pesant, S., Sullivan, M. B., Wincker, P., de Vargas, C., and Tara Oceans, C.: Tara Oceans: towards global ocean ecosystems biology, *Nature Reviews Microbiology*, 18, 428-445, 10.1038/s41579-020-0364-5, 2020.
- 855 Swadling, K. M., Constable, A. J., Fraser, A. D., Massom, R. A., Borup, M. D., Ghigliotti, L., Granata, A., Guglielmo, L., Johnston, N. M., Kawaguchi, S., Kennedy, F., Kiko, R., Koubbi, P., Makabe, R., Martin, A., McMinn, A., Moteki, M., Pakhomov, E. A., Peeken, I., Reimer, J., Reid, P., Ryan, K. G., Vacchi, M., Virtue, P., Weldrick, C. K., Wongpan, P., and Wotherspoon, S. J.: Biological responses to change in Antarctic sea ice habitats, *Frontiers in Ecology and Evolution*, 10, 10.3389/fevo.2022.1073823, 2023.
- 860 Tagliabue, A., Aumont, O., DeAth, R., Dunne, J. P., Dutkiewicz, S., Galbraith, E., Misumi, K., Moore, J. K., Ridgwell, A., Sherman, E., Stock, C., Vichi, M., Völker, C., and Yool, A.: How well do global ocean biogeochemistry models simulate dissolved iron distributions?, *Global Biogeochemical Cycles*, 30, 149-174, <https://doi.org/10.1002/2015GB005289>, 2016.



- 865 Tagliabue, A., Kwiatkowski, L., Bopp, L., Butenschön, M., Cheung, W., Lengaigne, M., and Vialard, J.: Persistent uncertainties in ocean net primary production climate change projections at regional scales raise challenges for assessing impacts on ecosystem services, *Frontiers in Climate*, 3, 2021.
- Timmermans, K. R., van der Wagt, B., and de Baar, H. J. W.: Growth rates, half-saturation constants, and silicate, nitrate, and phosphate depletion in relation to iron availability of four large, open-ocean diatoms from the Southern Ocean, *Limnology and Oceanography*, 49, 2141-2151, DOI 10.4319/lo.2004.49.6.2141, 2004.
- 870 Tortell, P. D., Payne, C. D., Li, Y., Trimborn, S., Rost, B., Smith, W. O., Riesselman, C., Dunbar, R. B., Sedwick, P., and DiTullio, G. R.: CO₂ sensitivity of Southern Ocean phytoplankton, *Geophysical Research Letters*, 35, <https://doi.org/10.1029/2007GL032583>, 2008.
- Touzé-Peiffer, L., Barberousse, A., and Le Treut, H.: The Coupled Model Intercomparison Project: History, uses, and structural effects on climate research, *Wiley Interdisciplinary Reviews: Climate Change*, 11, e648, 2020.
- 875 Tréguer, P., Bowler, C., Moriceau, B., Dutkiewicz, S., Gehlen, M., Aumont, O., Bittner, L., Dugdale, R., Finkel, Z., Iudicone, D., Jahn, O., Guidi, L., Lasbleiz, M., Leblanc, K., Levy, M., and Pondaven, P.: Influence of diatom diversity on the ocean biological carbon pump, *Nature Geoscience*, 11, 27-37, 10.1038/s41561-017-0028-x, 2018.
- Turner, J., and Comiso, J.: Solve Antarctica's sea-ice puzzle, *Nature*, 547, 275-277, 10.1038/547275a, 2017.
- 880 Turner, J., Holmes, C., Harrison, T. C., Phillips, T., Jena, B., Reeves-Francois, T., Fogt, R., Thomas, E. R., and Bajish, C. C.: Record Low Antarctic Sea Ice Cover in February 2022, *Geophysical Research Letters*, 49, e2022GL098904, ARTN e2022GL098904
10.1029/2022GL098904, 2022.
- Venables, H. J., Clarke, A., and Meredith, M. P.: Wintertime controls on summer stratification and productivity at the western Antarctic Peninsula, *Limnology and Oceanography*, 58, 1035-1047, <https://doi.org/10.4319/lo.2013.58.3.1035>, 2013.
- Virtanen, P., Gommers, R., Oliphant, T. E., Haberland, M., Reddy, T., Cournapeau, D., Burovski, E., Peterson, P., Weckesser, W., and Bright, J.: SciPy 1.0: fundamental algorithms for scientific computing in Python, *Nature methods*, 17, 261-272, 2020.
- 890 Ward, B. A., and Follows, M. J.: Marine mixotrophy increases trophic transfer efficiency, mean organism size, and vertical carbon flux, *Proceedings of the National Academy of Sciences*, 113, 2958-2963, doi:10.1073/pnas.1517118113, 2016.
- Watson, A. J., Bakker, D. C. E., Ridgwell, A. J., Boyd, P. W., and Law, C. S.: Effect of iron supply on Southern Ocean CO₂ uptake and implications for glacial atmospheric CO₂, *Nature*, 407, 730-733, 10.1038/35037561, 2000.
- 895 Weber, T. S., and Deutsch, C.: Ocean nutrient ratios governed by plankton biogeography, *Nature*, 467, 550-554, 10.1038/nature09403, 2010.



- Westwood, K. J., Thomson, P. G., van den Enden, R. L., Maher, L. E., Wright, S. W., and Davidson, A. T.:
Ocean acidification impacts primary and bacterial production in Antarctic coastal waters during austral summer,
900 *Journal of Experimental Marine Biology and Ecology*, 498, 46-60, <https://doi.org/10.1016/j.jembe.2017.11.003>,
2018.
- Wright, S. W., van den Enden, R. L., Pearce, I., Davidson, A. T., Scott, F. J., and Westwood, K. J.:
Phytoplankton community structure and stocks in the Southern Ocean (30–80 E) determined by CHEMTAX
analysis of HPLC pigment signatures, *Deep Sea Research Part II: Topical Studies in Oceanography*, 57, 758-778,
905 2010.
- Xu, K., Fu, F.-X., and Hutchins, D. A.: Comparative responses of two dominant Antarctic phytoplankton taxa to
interactions between ocean acidification, warming, irradiance, and iron availability, *Limnology and
Oceanography*, 59, 1919-1931, <https://doi.org/10.4319/lo.2014.59.6.1919>, 2014.
- Zhu, Z., Xu, K., Fu, F., Spackeen, J. L., Bronk, D. A., and Hutchins, D. A.: A comparative study of iron and
910 temperature interactive effects on diatoms and *Phaeocystis antarctica* from the Ross Sea, Antarctica, *Marine
Ecology Progress Series*, 550, 39-51, 2016.
- Zhuang, J., Dussin, R., Jüling, A., and Rasp, S.: xESMF: Universal regridding for geospatial data, Zenodo [code],
10, 2018.